Acta Pharmaceutica Sinica B 2019;9(2):351–368

Chinese Pharmaceutical Association
Institute of Materia Medica, Chinese Academy of Medical Sciences

Acta Pharmaceutica Sinica B

www.elsevier.com/locate/apsb
www.sciencedirect.com

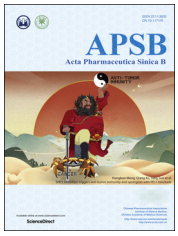

ORIGINAL ARTICLE

Discovery of a series of dimethoxybenzene FGFR inhibitors with 5*H*-pyrrolo[2,3-*b*]pyrazine scaffold: structure–activity relationship, crystal structural characterization and *in vivo* study

Peng Wei[a,b,†], Bo Liu[c,†], Ruifeng Wang[a,b], Yinglei Gao[c], Lanlan Li[c], Yuchi Ma[b], Zhiwei Qian[b], Yuelei Chen[b], Maosheng Cheng[a], Meiyu Geng[c], Jingkang Shen[b], Dongmei Zhao[a,*], Jing Ai[c,*], Bing Xiong[b,*]

[a]*Key Laboratory of Structure-Based Drug Design and Discovery of Ministry of Education, Shenyang Pharmaceutical University, Shenyang 110016, China*
[b]*Department of Medicinal Chemistry, Shanghai Institute of Materia Medica, Chinese Academy of Sciences, Shanghai 201203, China*
[c]*Division of Anti-tumor Pharmacology, State Key Laboratory of Drug Research, Shanghai Institute of Materia Medica, Chinese Academy of Sciences, Shanghai 201203, China*

Received 15 August 2018; received in revised form 9 November 2018; accepted 14 November 2018

KEY WORDS

Fibroblast growth factor;
Tyrosine kinase receptor;
Structure-based;
Crystallography;
Selectivity;
Hybrid;
5-Hydrosulfonyl-5*H*-pyrrolo[2,3-*b*]pyrazine;
Inhibitor

Abstract Genomic alterations are commonly found in the signaling pathways of fibroblast growth factor receptors (FGFRs). Although there is no selective FGFR inhibitors in market, several promising inhibitors have been investigated in clinical trials, and showed encouraging efficacies in patients. By designing a hybrid between the FGFR-selectivity-enhancing motif dimethoxybenzene group and our previously identified novel scaffold, we discovered a new series of potent FGFR inhibitors, with the best one showing sub-nanomolar enzymatic activity. After several round of optimization and with the solved crystal structure, detailed structure–activity relationship was elaborated. Together with *in vitro* metabolic stability tests and *in vivo* pharmacokinetic profiling, a representative compound (**35**) was selected and tested in xenograft mouse model, and the result demonstrated that inhibitor **35** was effective against tumors with FGFR genetic alterations, exhibiting potential for further development.

*Corresponding authors.
E-mail addresses: Zhaodm@syphu.edu.cn (Dongmei Zhao), jai@simma.c.cn (Jing Ai), bxiong@simm.ac.cn (Bing Xiong).
†These authors made equal contributions to this work.

Peer review under responsibility of Institute of Materia Medica, Chinese Academy of Medical Sciences and Chinese Pharmaceutical Association.

https://doi.org/10.1016/j.apsb.2018.12.008

1. Introduction

Phenotypic and genetic alternations associated with tumorigenesis were gradually uncovered by large scale applications of gene sequencing and proteomics approaches[1–3]. Along with these genomics-wide studies, we have witnessed the spurt of kinase inhibitors developed for targeted cancer treatment. Currently, more than 38 kinase drugs were approved by U.S. Food and Drug Administration (FDA), and most of them are targeting receptor tyrosine kinases[4–6]. However, cancer is a complex neoplasia, processing extensive phenotypic heterogeneity and numerous genetic and transcriptional variations[7–10]. Therefore, continuous efforts are needed to develop novel drugs as precision medicine for cancer patients.

Over the last years, the signaling pathways initialized by fibroblast growth factors (FGFs) are found to be important for progression and development of several cancers[11–14]. To the best of our knowledge, currently 18 FGFs are identified in human genome, which regulated by four transmembrane FGF receptors to transduce the signal to intracellular components. FGFRs belong to the receptor tyrosine kinase family, and each composes of three extracellular immunoglobin type domains and intracellular kinase domain. Canonically, once the ligand bind to FGFR causes the dimerization and autophsphorylation, and activation. Helsten et al.[15] analyzed frequencies of FGFR aberrations in 4853 solid tumors with next-generation sequencing, revealing that 7.1% of all tumor types have genetic alterations in the FGF–FGFR axis, among them 49% affects FGFR1, 19% affects FGFR2 and 23% affects FGFR3[15]. This, along with other evidences[16,17], reinforces that the FGFRs are promising targets for many types of cancer disease.

Currently, the FGFR small-molecule inhibitors all targeted the ATP binding site in kinase domain, and are roughly classified into two types, non-selective FGFR inhibitors and selective FGFR inhibitors[18]. As exemplified in Fig. 1, non-selective FGFR inhibitors are type-II kinase inhibitors, and usually associated with multi-kinase inhibitory activities, such as ponatinib which harbors potent activities at least for BCR-ABL, PDGFR, FGFR, VEGFR, and c-Src[19]. However, recent trend focused on developing selective FGFR inhibitors that are thought to have better safety window, and two most advanced drug candidates are illustrated in Fig. 1[20]. AZD4547, a potent FGFR1–3 inhibitor[21], showed strong inhibition on the FGFR downstream pathway and cytotoxic effects on multiple cell lines, including NSCLC cells with FGFR1 amplification, gastric cancer (GC) cells carrying the FGFR2 amplification and endometrial cell line harboring the FGFR2-K310R/N550K mutations. Appealing clinical trial data from phase II proof-of-concept study also indicated its efficacy in patients with FGFR2 amplified GC (RR 33%), enabling the candidate advanced to phase III. Similarly, ARQ-087[22], an oral pan-FGFR inhibitor, is also in phase III study, holding the promise for the treatment of patients with FGFR alterations.

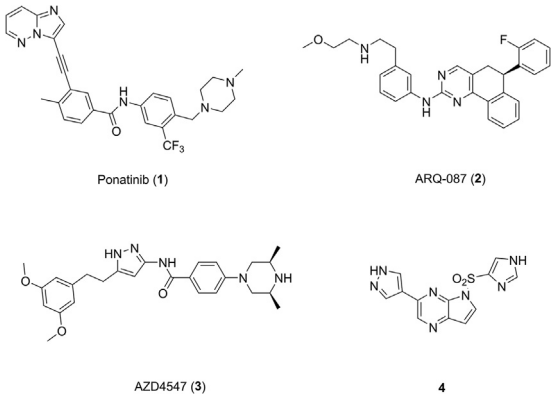

Figure 1 Representative FGFR inhibitors used in clinical trials (**1**–**3**) and our previous reported FGFR inhibitor (**4**).

In the present study, we reported our continuous effort on developing potent and selective FGFR inhibitors. Based on previous discoveries[23], we found 5-hydrosulfonyl-5*H*-pyrrolo[2,3-*b*]pyrazine (**4**) was an intriguing scaffold for FGFR inhibitors, as it can be used to install two parts of chemical groups, one for the back-pocket and another for the ribose pocket. And both of them are considered to be essential for selectivity. With the guidance of structure analysis, we rapidly optimized the enzymatic activity of this series to about 10 nmol/L. However, the poor *in vitro* metabolic stability of compounds in liver microsome and high P450 inhibition hinder the further evaluation. Based on the solved crystal structure and metabolite identification, we carried out the optimization and finally obtained inhibitor **35** through the *in vivo* pharmacokinetic study as the promising FGFR inhibitor. Further *in vivo* pharmacological study confirmed the utility of the compound.

2. Results and discussion

2.1. Ligand design with hybrid approach

Based on our previous reported scaffold (5-hydrosulfonyl-5*H*-pyrrolo [2,3-*b*]pyrazine), we firstly carried out the structure-based binding mode analysis by superimposing cocrystal structure containing this scaffold (PDB 5Z0S)[23] and cocrystal structure AZD4547 (PDB 4V05)[24]. Clearly, based on the hybrid idea, we can substitute the pyrazole with two carbon linker and dimethoxybenzene group, which will extend into back pocket to make more favorable van der Waals interactions with the surrounding residues, thus increasing the binding affinity. Since in crystal structure 5Z0S the 6-chloroimidazo[1,2-*b*] pyridazine group forms a π–π stacking interaction with residue Phe489, we intended to preserve this interaction but to simplify the synthesis. Therefore, a synthesis-accessible benzene group was used to quickly test the hypothesis about the substitution with dimethoxybenzene group.

As listed in Table 1, compound **5** showed about 75% inhibition ratio at 0.1 μmol/L, indicating the dimethoxybenzene is a better option for optimization. Dichloro substitution on the dimethoxybenzene (**7**) further increased the inhibitory activity to 14 nmol/L. Interestingly, modifying the linker can influence the binding activity: changing a carbon to nitrogen decreased the binding

activity; using ethylene rigidifies the linker can retain the activity, while using the acetylene decreased the activity about 10 folds.

2.2. *Optimization of imidazole part*

After confirming dimethoxybenzene is a suitable back-pocket binding motif, we proceeded to optimize the π–π stacking group. As shown in Table 2, substitution with cyclopentane ring (**10**) reduced the binding activity, which supports that it needs an aromatic ring system to participate in the π–π stacking. Generally, comparing bicyclic compounds (**17**–**19**), we found that monocyclic aromatic compounds showed better binding activities. However, compounds substituted with electron-deficient ring (**11**) or electron-rich ring (**12**) displayed similar binding activities, indicating the electron property is not a relevant factor for the binding. Comparing compounds **15** and **16**, we can realize that compounds substituted at *para*-position of benzene group generate more potent inhibitors.

To verify the binding mode of this series of inhibitors, we conducted crystallization of FGFR2 with compound **14**. As illustrated in Fig. 2B, the dimethoxybenzene group situated in the back pocket, making van der Waals interactions with surrounding residues Met538, Val564 and Phe645 and the imidazole positioned above the pyrrolopyrazine scaffold. However, different from the prediction, the imidazole did not form π–π stacking with the protein. Besides, we found the A-loop of FGFR2 kinase domain was disordered in current crystal structure. Whether this discrepancy is due to the difference between FGFR1 and FGFR2 or is due to different ligands still needs further investigation. The ethyl acetate substitution on the imidazole group oriented into the back pocket, making a weak hydrogen bonding interaction with the backbone of residue Asp644 (the distance between heavy atoms is 3.2 Å).

Based on the solved crystal structure (5Z0S), we speculated that the imidazole of compound **12** would be facing the interior part of the binding site. Therefore, it may provide new direction for next round optimization. The inhibitory activity of compound **14** further strengthened this hypothesis. Then, we selected compound **12** to check its metabolic stability, as it represents the simple starting point for further optimization. As listed in Table 4, this compound showed good stability in human microsome. But from the CYP450 inhibition assay, it turned out to be a potent inhibitor for five isotype CYP450 enzymes, indicative of a potential drug–drug interaction risk, which makes us to perform further optimization.

Based on the solved crystal structure of **14**, we decided to focus on the imidazole part, as it has large room for modification. As shown in Table 3, compounds with various substitutions on imidazole ring were prepared and several of them showed excellent inhibitory activities

Table 1 The FGFR1 enzymatic activities of compounds **5**–**9**[a].

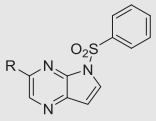

Compd.	R	FGFR1 inhibition ratio (%)			
		1 μmol/L	0.1 μmol/L	0.01 μmol/L	IC_{50} (nmol/L)
5	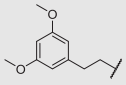	95	75	40.3	–
6	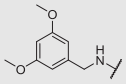	74.8	34.8	–	–
7	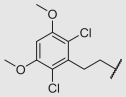	94.0	91.8	–	14.8±3.4
8	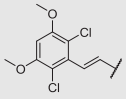	96.3	78.4	–	12.0±3.3
9	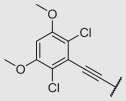	59.3	51.0	–	145.2±13.2

–, not tested.

[a]Inhibition ratio and IC_{50} values are given as the mean from three separate experiments.

Table 2 The FGFR1 enzymatic activities of compounds **10–19**[a].

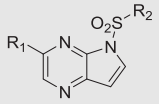

Compd.	R_1	R_2	FGFR1 inhibition ratio (%)	
			100 nmol/L	10 nmol/L
10	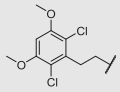		60.0	33.7
11	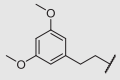		90.7	80.4
12	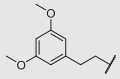		88.2	69.6
13	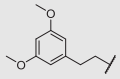		87.5	63.9
14	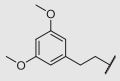	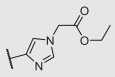	96.9	78.5
15	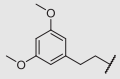		79.5	62.2
16	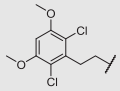		82.3	52.1
17	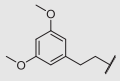		63.3	45.8
18	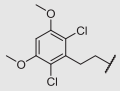		85.9	54.9
19	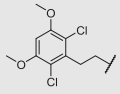		59.2	34.5

[a]Inhibition ratio are given as the mean from three separate experiments.

towards FGFR1 enzymatic assay and FGFR1-amplification KG1 cellular assay. Detailed analysis identified that the smaller the substituents the higher the inhibitory activity. For example, compounds **20** and **21** with small substituents exhibited single digit nanomolar activity. While several bulky substituents (**25–28**) showed much lower inhibitions, which may clash with surrounding residues and reduce the binding affinity. We also synthesized compound **29** containing 1,5-dichloro-2,4-dimethoxybenzene to check the binding affinity. The result indicated it is a very potent FGFR1 inhibitor, with the enzymatic IC_{50} value in the picomolar range. We also tested the antiproliferative activity of these compounds in KG1 cellular context. In consistent with the enzymatic assay, compounds with smaller substituents showed great antiproliferative inhibition. However, compound **29** did not present highest cellular activity, which may be due to the compound is more hydrophilic than other analogues (**20–22**). Therefore, it is detrimental to the membrane permeability.

2.3. *Optimization of metabolic stability*

We selected three potent inhibitors to check the metabolic stability. As listed in Table 4, similar to compound **12**, compound **29** still

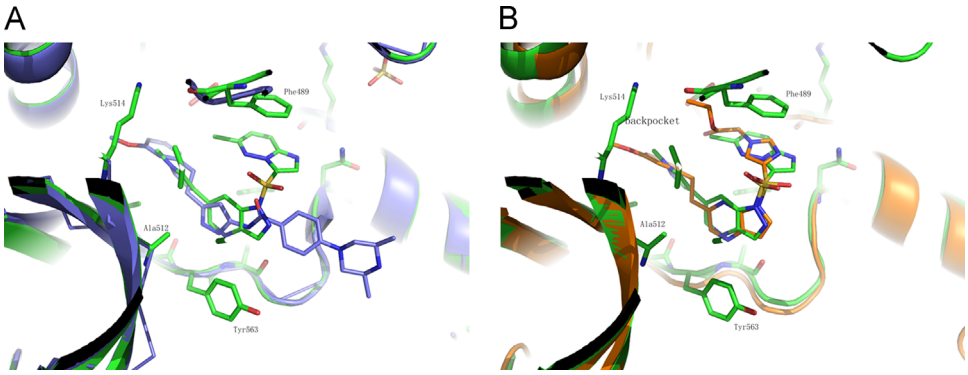

Figure 2 Superimposition of cocrystal structure of FGFR inhibitors, and the protein are shown in cartoon style and ligands are illustrated in stick model. (A) alignment of our previous solved crystal structure (PDB 5Z0S, carbon atoms are colored in green) and AZD4547 (PDB 4V05, carbon atoms are colored in blue). (B) alignment of our previous solved crystal structure (PDB 5Z0S, carbon atoms are colored in green) and present solved crystal structure of compound **14** (PDB 6AGX, carbon atoms are colored in orange).

showed high inhibition towards five CYP450 enzymes. However, the substituted imidazole compounds appear reduced inhibitory activities on CYPs, and only the CYP450 3A4 was targeted with about 90% inhibition ratio at 10 μmol/L concentration. To find out the metabolic liable site of the inhibitors, we picked compound **21** to perform the metabolite identification. The result demonstrated that demethylation at dimethoxybenzene ring is the main factor contributing to the metabolism of this compound in human liver microsome (Supporting Information Fig. S1).

Consequently, the next round of optimization focused on the dimethoxybenzene ring. To reduce the rate of demethylation, two approaches were adopted. The first is to modify the methoxyl group by extending to ethyl (**30**) or cyclizing (**31**). However, the inhibitory activity decreased dramatically. It is known that electron-rich chacteristics will enable the P450 enzyme to accelerate the metabolic catalysis. Thus, the second approach is to reduce the electron density of dimethoxybenzene by adding the fluorine atom (**32**), which slightly increased the IC_{50} activity to 0.4 nmol/L. We further prepared three analogues by changing the substituents on imidazole (**33**) and modifying the linker to ethylene to further rigidify the compounds (**34** and **35**). The three compounds showed equipotent enzymatic activity as compound **32**. The antiproliferative inhibition on KG1 cell line of these four fluorine substituents were also listed in Table 5, demonstrating high potency as FGFR1 inhibitors.

In order to verify the utility of this series of FGFR inhibitors, compound **35** was selected for metabolic stability test, as it processing excellent potency, lower electron density on dimethoxybenzene moiety and possibly stabilized fluoroethyl substituted imidazole ring. As shown in Table 4, compound **35** demonstrated much lower inhibition ratio for five selected CYPs than previous tested compounds.

Before investigating the antitumor activity of compound **35**, we selected 12 typical RTKs to assess its kinase selectivity. The data (Supporting Information Table S2) showed that compound **35** has negligible inhibition on these kinases, indicating compound **35** is a selective FGFR inhibitor. We also inspected the pharmacokinetic properties of compound **35** in mice. Three CD-1 mice were dosed with 10 mg/kg of **35** *via* intragastric administration. From the calculated PK parameters, it was found the compound has moderate plasma exposure (AUC 434 ng · h/mL) and half-life of 1.9 h. Given the maximum drug concentration in plasma of about 342 ng/mL and lipophilic characteristics of **35**, we speculated the compound may have good tissue distribution. We continued the *in vivo* pharmacological study to check the antitumor effect of **35**.

2.4. *In vivo antitumor efficacy of compound 35*

We assessed the *in vivo* efficacies of **35** on model with FGFR alterations. Mice bearing xenograft tumors derived from SNU-16 cells (this cell line is FGFR2-amplified, and IC_{50} of compound **35** against this cell line is 74.8 nmol/L), as the representative model, was treated orally with **35** once daily for 21 consecutive days. As illustrated in Fig. 3, **35** suppressed the tumor growth at a dose of 10 mg/kg in the SNU-16 model (Fig. 3A). No severe weight loss was observed during the treatment (Fig. 3B). These results demonstrated that inhibitor **35** was effective against tumors with FGFR genetic alterations, exhibiting potential for further study.

2.5. *Chemistry*

Compounds **5**–**7** and **10**–**29** were prepared according to Scheme 1. Sonogashira coupling of **36** with TMSA provided **37**. Intramolecular ring of **37** produced **38.** Treatment of **38** with benzenesulfonyl chloride afforded **39,** and Buchwald–Hartwig coupling reaction with corresponding amine was used to generate **6**. Sonogashira coupling of **38** with 3,5-dimethoxyphenylacetylene provided **40**. Compound **40** was reduced with Pd–C under 2 bar H_2 to **41**. Treatment of **41** with corresponding benzenesulfonyl chloride afforded **11**–**13**, **17**, **20**, **21** and intermediate **42**. Compound **42** was reduced with iron powder to **43**. Treatment of **43** with acetyl chloride afforded **15**. Compounds **14**, **22**–**28** were prepared by substitution of **12** with corresponding halide. Compound **41** were sulfonylated to afford **5**, and treatment of **5** with sulfuryl dichloride afforded **7**. Compound **44** was generated by the removal of benzyl sulfonyl. Treatment of **67** with sulfurochloridic acid afforded **68**. Compound **69** was generated by the reaction of **68** with PCl_5. Compound **44** were sulfonylated to afford **10**, **18**, **19**, **29** and intermediate **45**. Compound **45** was reduced with iron powder to **46** and **16** was synthesized with acetyl chloride.

Compounds **8**, **9**, **30**, and **31** were prepared according to the procedures in Scheme 2. Sonogashira coupling of **47** with TMSA provided **48**; treatment of **48** with sulfuryl dichloride afforded **49**; compound **50** was generated by the removal of silicon protection; Sonogashira coupling conditions were used to generate

Table 3 The FGFR1 enzymatic and antiproliferative activities of compounds **20–29**[a].

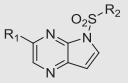

Compd.	R_1	R_2	FGFR1 inhibition ratio (%)			KG1 inhibition
			100 nmol/L	10 nmol/L	IC_{50} (nmol/L)	IC_{50} (nmol/L)
20	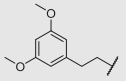		96.9	82.3	1.3±0.2	3.4±0.1
21	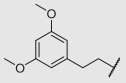		89.5	64.0	1.2±0.7	1.4±0.5
22	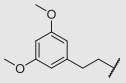		89.8	71.7	3.4±0.8	2.1±0.0
23	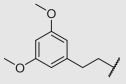		72.4	41.4	18.9±4.0	>1000
24	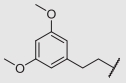		88.2	51.4	–	>1000
25	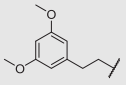	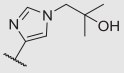	66.2	34.0	–	>1000
26	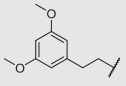	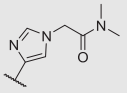	52.2	38.9	–	>1000
27	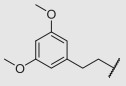	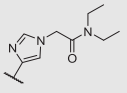	10.3	38.7	820.1±160.0	>1000
28	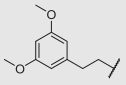	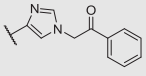	46.3	32.7	–	>1000
29	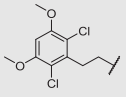		99.7	94.3	<0.03	20.6±5.3

–, not tested.

[a]Inhibition ratio and IC_{50} values are given as the mean from three separate experiments.

9. Treatment of **51** with sulfuryl dichloride afforded **52**. Compound **53** was prepared by Wittig reaction of **52**, and Heck coupling conditions were used to generate **8**. Sonogashira coupling of **38** provided **54a** and **54b**. Compounds **54a** and **54b** were reduced and sulfonylated to afford **30** and **31**.

Compounds **32–35** were synthesized according to the procedures in Scheme 3. Compound **56** was generated by the removal of silicon protection of **48**. Treatment of **56** with Selectflour afforded **57** and **58**. Sonogashira coupling of **38** provided **59**. Compound **59** was reduced and sulfonylated to afford **32**. Compound **38** was sulfonylated to afford **61** and **63**. Sonogashira coupling of **61** afforded **62**. Compound **34** was synthesized by reduction. Compound **64** was provided by substitution of **63**, and Sonogashira coupling conditions were used to provide **65** and **66**. Compounds **33** and **35** were prepared by reduction.

3. Conclusions

Aberrant signaling of FGF–FGFR axis was identified in many types of human cancers, which stimulates extensive efforts to develop inhibitors targeting the FGFR, a subfamily of receptor tyrosine kinases. Based on

Table 4 *In vitro* metabolic stability assay and P450 inhibition profile.

Compd.	HLM[a] Cl (int, app) [uL/min/mg]	CYPs Direct inhibition (%)[b]					TDI[c]
		3A4	2D6	2C9	1A2	2C19	
12	38	96	90	97	60	99	No inhibition
20	212	88	–	–	32	7	3A4, 1A2
21	54	94	15	52	58	42	3A4
29	50	90	78	99	59	99	No inhibition
35	100	71	9	21	28	3	No inhibition

–, not tested.

[a]Human liver microsomal intrinsic clearance (μL/min · mg).

[b]CYPs direct inhibition, sometimes referred to reversible inhibition, is assessed by measurement of an enzyme (CYP) activity in the presence of increasing concentration of inhibitor without a pre-incubation step.

[c]TDI stands for time-dependent inhibition, which is referring to a change in enzyme inhibition during an *in vitro* incubation and means an irreversible inactivation of CYPs. The k_{obs} value lower than 200 (unit: 10^{-4}/min) was considered to be no TDI inhibition.

Table 5 The FGFR1 enzymatic and antiproliferative activities of compounds **30–35**[a].

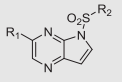

Compd.	R_1	R_2	FGFR1 inhibition ratio (%)			KG1 inhibition
			100 nmol/L	10 nmol/L	IC_{50} (nmol/L)	IC_{50} (nmol/L)
30	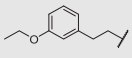		44.2	69.9	103.3±30.5	25.9±4.5
31	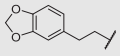		33.7	51.0	–	–
32	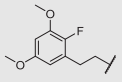		99.7	92.4	0.4±0.1	<0.3
33	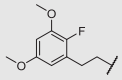	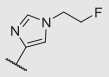	96.1	84.9	0.2±0.07	<0.3
34	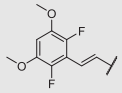		101.6	96.6	0.8±0.1	<0.3
35	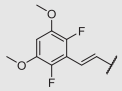	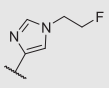	95.1	75.9	0.6±0.0	0.5±0.3

–, not tested.

[a]Inhibition ratio and IC_{50} values are given as the mean from three separate experiments.

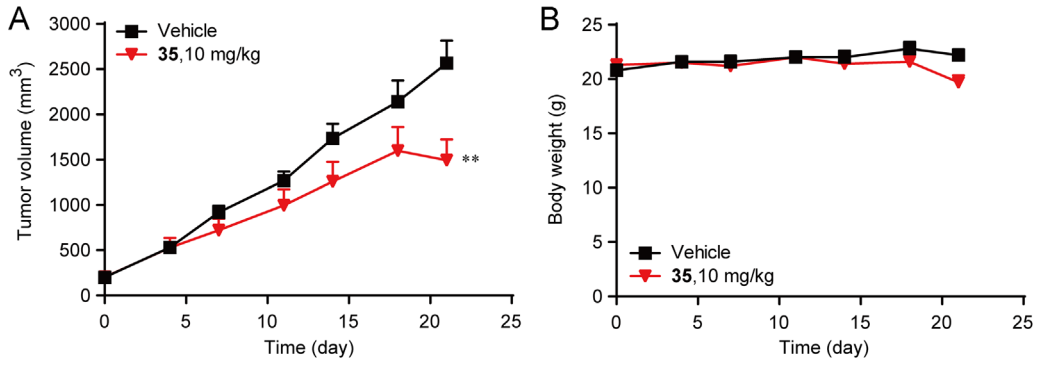

Figure 3 Compound **35** significantly inhibited FGFR-mediated tumor growth *in vivo*. (A) Tumor growth was inhibited upon **35** treatment in SNU–16 xenografts. The RTVs are expressed as the mean ± SEM. Significant difference from the vehicle group was determined using a Student's *t*-test, $n = 6$, $^{**}P < 0.01$. (B) Body weight measurements during treatment.

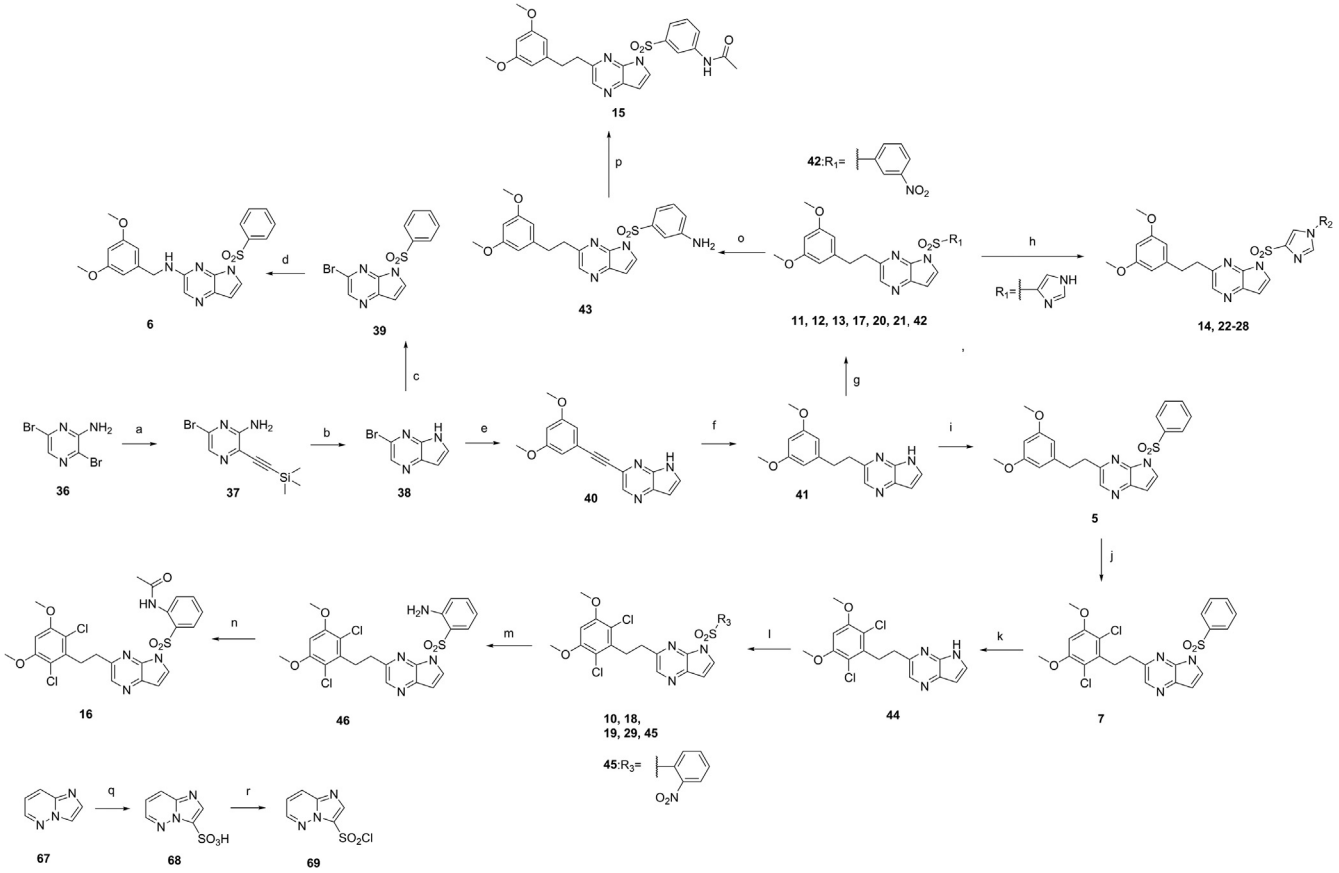

Scheme 1 The synthesis of the compounds **5–7** and **10–29**. Reagents and conditions:(a) TMSA, $Pd(PPh_3)_2Cl_2$, CuI, TEA, THF, N_2, 0 °C–r.t.; (b) *t*-BuOK, DMF, 0 °C–r.t., overnight; (c) benzenesulfonyl chloride, NaH, DMF, 0 °C–r.t.; (d) (3,5-dimethoxyphenyl)methanamine, $Pd_2(dba)_3$, BINAP, Cs_2CO_3, toluene, 100 °C, 3 h; (e) 3,5-dimethoxyphenylacetylene, $Pd(PPh_3)_2Cl_2$, CuI, TEA, DMF, 80 °C, 3–4 h; (f) dry Pd–C, 30 °C, 2 bar H_2, EtOH, 4 h; (g) corresponding sulfonyl chloride, NaH, DMF, 0 °C–r.t.; (h) corresponding halide, K_2CO_3, DMF, 60 °C, 2 h; (i) benzenesulfonyl chloride, NaH, DMF, 0 °C–r.t.; (j) sulfuryl dichloride, DCM, 0 °C, 30 min; (k) TBAF, THF, 50 °C, 5 h; (l) corresponding sulfonyl chloride, NaH, DMF, 0 °C–r.t.; (m) Fe, HCl, EtOH, reflux, 4 h; (n) acetyl chloride, DMAP, DIPEA, DCM, 0 °C, 30 min; (o) Fe, HCl, EtOH, reflux, 4 h; (p) acetyl chloride, DMAP, DIPEA, DCM, 0 °C, 30 min; (q) chlorosulfonic acid, $CHCl_3$, reflux, 20 h; (r) $POCl_3$, PCl_5, reflux, 8 h.

the hybrid approach and structure-based design, we combined a novel scaffold and a well-known FGFR-selectivity enhancing motif to quickly optimize the enzymatic activity to nmol/L range. With considerable efforts to improve the drug-like properties, we finally obtained a potent and *in vivo* active compound showing a promising sign for further development. Although there are several selective FGFR inhibitors currently being investigated in clinical trials, they may have different response to various mutated FGFR kinases. Also,

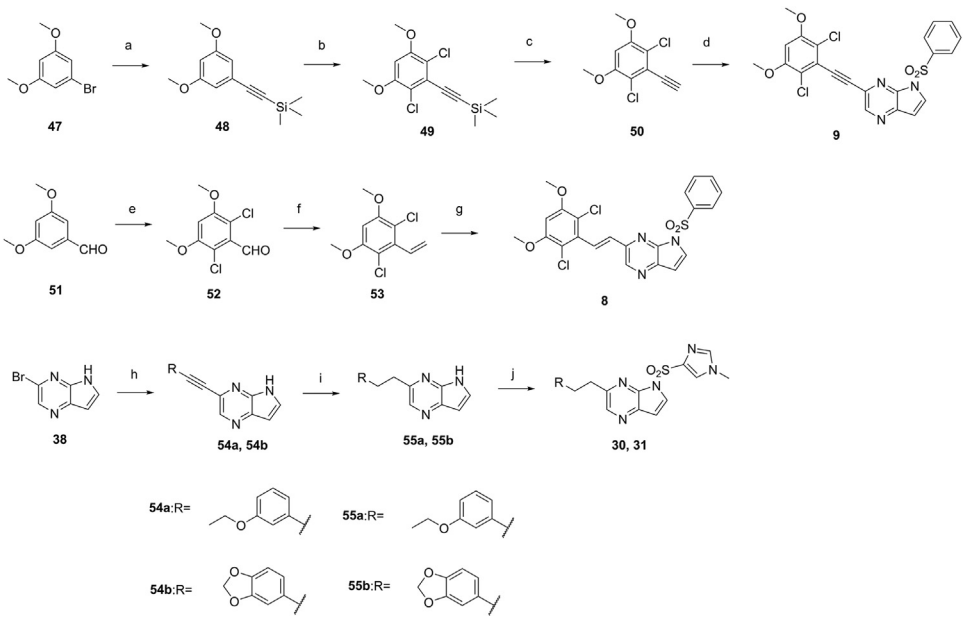

Scheme 2 The synthesis of the compounds **8, 9** and **30, 31**. Reagents and conditions:(a) TMSA, $Pd(PPh_3)_2Cl_2$, CuI, TEA, DMF, N_2, 80 °C, 4 h; (b) sulfuryl dichloride, DCM, 0 °C, 3 h; (c) TBAF, THF, r.t., 2 h; (d) **39**, $Pd(PPh_3)_2Cl_2$, CuI, TEA, DMF, 80 °C, overnight; (e) sulfuryl dichloride, DCM, 0 °C, overnight; (f) Methyltriphenylphosphonium bromide, *t*-BuOK, THF, r.t., overnight; (g) **39**, $Pd(OAc)_2$, K_2CO_3, Ph_3P, DMA, 100 °C, overnight; (h) corresponding Phenylacetylene, $Pd(PPh_3)_2Cl_2$, CuI, TEA, DMF, 100 °C, 3–4 h; (i) Pd–C, 30 °C, 2 bar H_2, EtOH, 4 h; (j) 1-methyl-4-imidazole sulfonyl chloride, NaH, DMF, 0 °C–r.t.

acquired resistance to the kinase inhibitors make it inevitable to develop new chemotype inhibitors. Giving the novel binding mode of present disclosed FGFR inhibitors, it would be interesting to see whether it will have different utility in profiling the landscape of mutations of FGFRs, or it will play a different role in treating the acquired resistance coming along with other FGFR inhibitors.

4. Materials and methods

4.1. General methods of chemistry

^{1}H NMR (400 MHz) spectra were recorded by using a Varian Mercury-400 high performance digital FT-NMR spectrometer (Varian, Palo Alto, USA) with tetramethylsilane (TMS) as an internal standard. ^{13}C NMR (100 or 125 MHz) spectra were recorded by using a Varian Mercury-400 high performance digital FT-NMR spectrometer (Varian, Palo Alto, USA) or Varian Mercury-500 high performance digital FT-NMR spectrometer (Varian, Palo Alto, USA). Abbreviations for peak patterns in NMR spectra are the following: br = broad, s = singlet, d = doublet, and m = multiplet. Low-resolution mass spectra were obtained with a Finnigan LCQ Deca XP mass spectrometer (ThermoFinnigan, Santa Clara County, USA) using a CAPCELL PAK C18 (50 mm × 2.0 mm, 5 μm) or an Agilent ZORBAX Eclipse XDB C18 (50 mm × 2.1 mm, 5 μm) (Agilent, Santa Clara County, USA) in positive or negative electrospray mode. Low-resolution mass spectra and high-resolution mass spectra were recorded at an ionizing voltage of 70 eV on a Finnigan/MAT95 spectrometer (ThermoFinnigan, Santa Clara County, USA). High resolution mass spectra were recorded by using a Finnigan MAT-95 mass spectrometer (ThermoFinnigan, Santa Clara County, USA) or an Agilent technologies 6224 TOF mass spectrometer (Agilent, Santa Clara County, USA). Purity of all compounds was determined by analytical Gilson high performance–liquid chromatography (HP–LC) using an YMC ODS3 column (50 mm × 4.6 mm, 5 μm). Conditions were as follows: CH_3CN/H_2O eluent at 2.5 mL/min flow [containing 0.1% trifluoroacetic acid (TFA)] at 35 °C, 8 min, gradient 5% CH_3CN to 95% CH_3CN, monitored by UV absorption at 214 and 254 nm. TLC analysis was carried out with glass precoated silica gel GF254 plates. TLC spots were visualized under UV light (SCRC, Shanghai, China). Flash column chromatography was performed with a Teledyne ISCO CombiFlash Rf system (Teledyne, Santa Clara County, USA). All solvents and reagents were used directly as obtained commercially unless otherwise noted. Anhydrous dimethylformamide was purchased from Acros (InnoChem, Beijing, China) and was used without further drying. All air and moisture sensitive reactions were carried out under an atmosphere of dry argon with heat-dried glassware and standard syringe techniques. Microwave reactions were performed with Biotage initiator focused beam microwave reactor (400 W, Biotage, Stockholm, Biotage).

4.2. The synthesis of details of target compounds

*4.2.1. 6-Bromo-3-((trimethylsilyl)ethynyl)pyrazin-2-amine (**37**)*

3,6-Dibromopyrazin-2-amine (**36**, 5 g, 19.8 mmol), TMSA (2.14 g, 21.8 mmol), $Pd(PPh_3)_2Cl_2$ (1.15 g, 0.99 mmol), CuI (189 mg, 0.99 mmol) and triethylamine (4 g, 39.6 mmol) were dissolved in THF and the resultant solution was purged with argon. The reaction mixture was cooled to 0 °C and stirred for 1H. And then the reaction was left to warm up to room temperature for another 8 h. Then water was added to the reaction system. The reaction mixture was extracted with ethyl acetate. The organic phase was concentrated under reduced pressure to give the crude target product, which was purified by flash column chromatography with dichloromethane/methanol to afford compound

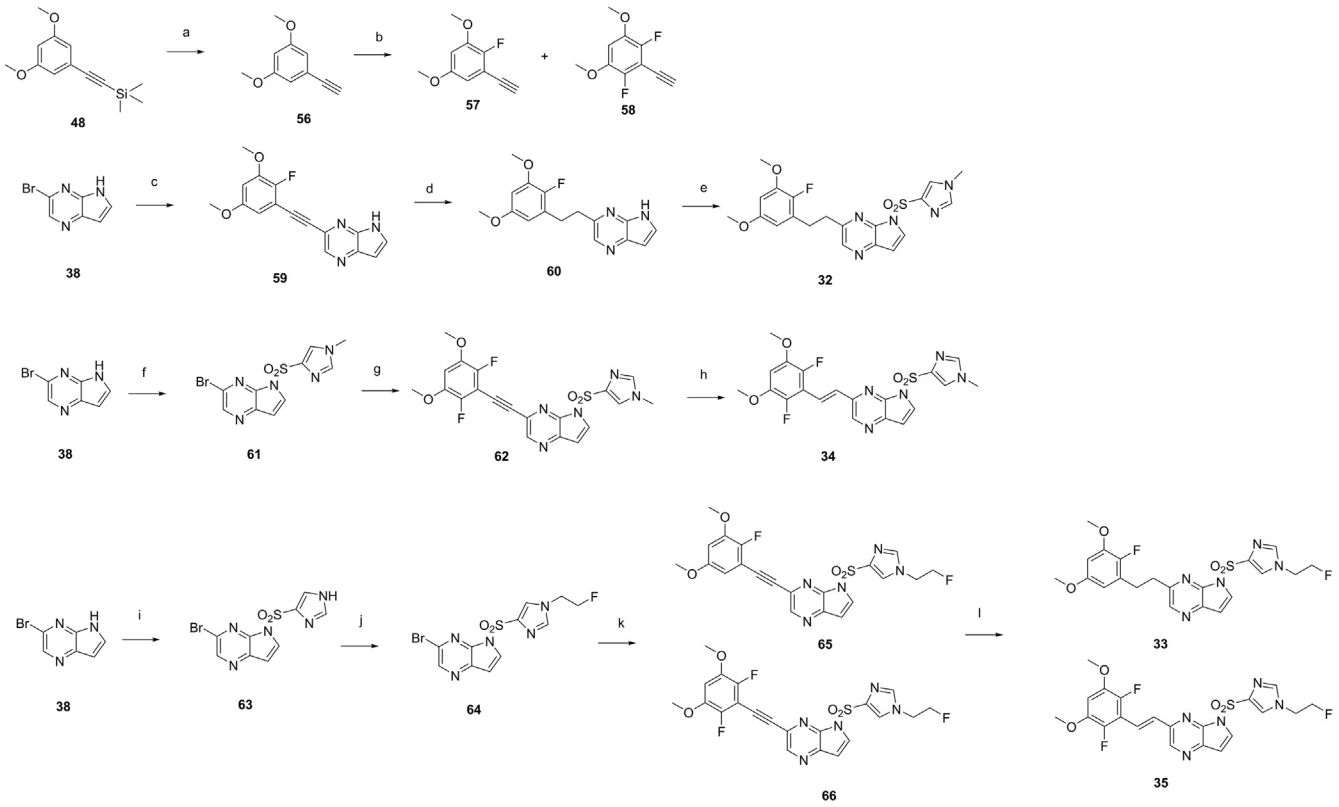

Scheme 3 The synthesis of the compounds **32–35**. Reagents and conditions:(a) TBAF, DCM, r.t., 1 h; (b) Selectflour, acetonitrile, 0 °C–r.t., overnight; (c) **57**, $Pd(PPh_3)_2Cl_2$, CuI, TEA, DMF, 80 °C, overnight; (d) H_2, $Pd(OH)_2$, EtOH, 50 °C, 6 h; (e) 1-methyl-4-imidazole sulfonyl chloride, NaH, DMF, 0 °C–r.t.; (f) 1-methyl-4-imidazole sulfonyl chloride, NaH, DMF, 0 °C–r.t.; (g) **57**, $Pd(PPh_3)_2Cl_2$, CuI, TEA, DMF, 80 °C, overnight; (h) H_2, $Pd(OH)_2$, 50 °C, EtOH, 6 h; (i) 4-imidazole sulfonyl chloride, NaH, DMF, 0 °C–r.t.; (j) 1-fluoro-2-iodoethane, K_2CO_3, DMF, 60 °C, 3 h; (k) **57** and **58**, $Pd(PPh_3)_2Cl_2$, CuI, TEA, DMF, 80 °C, overnight; (l) H_2, $Pd(OH)_2$, EtOH, 50 °C, 6 h.

37 as yellow solid with the yield of 71%. ^{1}H NMR (400 MHz, chloroform-*d*) δ 7.81 (s, 1H), 5.20 (s, 2H), 0.27 (s, 9H).

4.2.2. 3-Bromo-5H-pyrrolo[2,3-b]pyrazine (38)

6-Bromo-3-((trimethylsilyl)ethynyl)pyrazin-2-amine (**37**, 3 g, 11 mmol) was dissolved in anhydrous DMF and the mixture was cooled to 0 °C. Potassium *t*-butoxide (2.5 g, 22 mmol) was slowly added to the above solution. Then the mixture was stirred for 4 h at 0 °C. Subsequently, the reaction was stirred for another 20 h at room temperature. After the reaction finished (monitored by TLC), water was added. The mixture was extracted three times with ethyl acetate, washed with ammonium chloride and dried over sodium sulfate, concentrated, and purified by column chromatography to give compound **38** as yellow solid with the yield of 62%. ^{1}H NMR (400 MHz, DMSO-d_6) δ 12.32 (s, 1H), 8.52 (s, 1H), 7.92 (d, J = 3.6 Hz, 1H), 6.69 (d, J = 3.7 Hz, 1H).

4.2.3. 3-Bromo-5-(phenylsulfonyl)-5H-pyrrolo[2,3-b]pyrazine (39)

3-Bromo-5*H*-pyrrolo[2,3-b]pyrazine (**38**, 100 mg, 0.5 mmol) and NaH (13 mg, 0.55 mmol) were dissolved in anhydrous DMF. After the reaction mixture was stirred at 0 °C for 10 min. Benzenesulfonyl chloride (75 μL, 0.55 mmol) dissolved in 5 mL of anhydrous DMF was slowly added in drops, and the mixture was stirred for 1H at room temperature. The resulting solution was poured into H_2O and extracted with CH_2Cl_2. The organic layer was washed with brine and dried with Na_2SO_4. The organic phase was concentrated under reduced pressure. The residue was purified by flash chromatography to afford **39** as white solid with the yield of 88%. ^{1}H NMR (400 MHz, chloroform-*d*) δ 8.61 (s, 1H), 8.24 (dd, J = 8.5, 1.3 Hz, 2H), 7.99 (d, J = 4.1Hz, 1H), 7.71–7.64 (m, 1H), 7.62–7.55 (m, 2H), 6.83 (d, J = 4.1Hz, 1H).

4.2.4. N-(3,5-Dimethoxybenzyl)-5-(phenylsulfonyl)-5H-pyrrolo[2,3-b]pyrazin-3-amine (6)

3-Bromo-5-(phenylsulfonyl)-5*H*-pyrrolo[2,3-*b*]pyrazine (**39**, 100 mg, 0.296 mmol), 3,5-dimethoxybenzylamine (49 μL, 0.325 mmol), BINAP (18 mg, 0.03 mmol) and Cs_2CO_3 (193 mg, 0.59 mmol) were dissolved in methylbenzene in a microwave tube was flushed with N_2 for 5 min, then $Pd_2(DBA)_3$ (27 mg, 0.03 mmol) was added and the reaction was degassed again for further 5 min. The resulting mixture was stirred at 100 °C for 3 h. Then the reaction mixture was evaporated to dryness. The residue was purified by flash chromatography to give **6** as gray solid with the yield of 70%. ^{1}H NMR (400 MHz, chloroform-*d*) δ 8.06 (dd, ;J = 8.5, 1.2 Hz, 2H), 7.88 (s, 1H), 7.59–7.52 (m, 2H), 7.42–7.34 (m, 2H), 6.65 (d, J = 4.1Hz, 1H), 6.57 (d, J = 2.2 Hz, 2H), 6.44 (t, J = 2.2 Hz, 1H), 5.08 (s, 1H), 4.65 (d, J = 5.8 Hz, 2H), 3.81 (s, 6H). LC–MS (ESI): *m/z* 425.16 $[M+H]^+$. HPLC purity: >95%, retention time = 3.49 min. HR-MS *m/z* (ESI) Found 425.1271 $[M+H]^+$, $C_{21}H_{21}N_4O_4S^+$ Calcd. for 425.1278.

4.2.5. *3-((3,5-Dimethoxyphenyl)ethynyl)-5H-pyrrolo[2,3-b]pyrazine (**40**)*

A solution of 3-bromo-5*H*-pyrrolo[2,3-*b*]pyrazine (**38,** 100 mg, 0.51 mmol), 3,5-dimethoxyphenylacetylene (91 mg, 0.56 mmol), $Pd(PPh_3)_2Cl_2$ (58 mg, 0.05 mmol), CuI (10 mg, 0.05 mmol) and triethylamine (104 mg, 1.02 mmol) in DMF in a microwave tube was flushed with N_2 for 5 min then sealed. The tube was heated at 100 °C for 3 h. Then the reaction mixture was evaporated to dryness. The residue was purified by flash chromatography to give **40** as gray solid with the yield of 78%. ^{1}H NMR (400 MHz, DMSO-d_6) δ 12.22 (s, 1H), 8.64 (s, 1H), 8.07–7.99 (m, 1H), 6.81 (d, J = 2.2 Hz, 2H), 6.70 (dd, J = 3.5, 1.7 Hz, 1H), 6.62 (t, J = 2.2 Hz, 1H), 3.80 (s, 6H).

4.2.6. *3-(3,5-Dimethoxyphenethyl)-5H-pyrrolo[2,3-b]pyrazine (**41**)*

Hydrogen gas was applied (2 bar) onto a solution of 3-((3,5-dimethoxyphenyl)ethynyl)-5*H*-pyrrolo[2,3-*b*]pyrazine (**40**, 100 mg) and dry Pd–C (10 mg) in EtOH. Then the mixture was stirred for 4 h at 30 °C. After the reaction finished (monitored by TLC), the solid was separated by decantation and filtration. The liquid was concentrated under reduced pressure. The crude mixture was purified by flash column chromatography on silica gel to afford compound **41** as white solid with the yield of 92%. ^{1}H NMR (400 MHz, chloroform-*d*) δ 10.26 (s, 1H), 8.38 (s, 1H), 7.60–7.55 (m, 1H), 6.75 (dd, J = 3.6, 1.8 Hz, 1H), 6.40 (d, J = 2.1Hz, 2H), 6.34 (d, J = 2.1Hz, 1H), 3.77 (s, 6H), 3.26 (dd, J = 9.6, 6.4 Hz, 2H), 3.10 (dd, J = 9.4, 6.5 Hz, 2H).

4.2.7. *5-((1H-Imidazol-4-yl)sulfonyl)-3-(3,5-dimethoxyphenethyl)-5H-pyrrolo[2,3-b]pyrazine (**12**)*

3-(3,5-Dimethoxyphenethyl)-5*H*-pyrrolo[2,3-*b*]pyrazine (**41**, 1 g, 3.5 mmol) and NaH (93 mg, 3.85 mmol) was dissolved in anhydrous DMF. After the reaction mixture was stirred at 0 °C for 10 min. 1*H*-Imidazole-4-sulfonyl chloride was dissolved (641 mg, 3.85 mmol) in anhydrous DMF was slowly added in drops, and the mixture was stirred for 20 min at room temperature. Then the resulting solution was poured into H_2O and extracted with CH_2Cl_2. The organic layer was washed with brine and dried with Na_2SO_4. The organic phase was concentrated under reduced pressure. The residue was purified by flash chromatography to afford **12** as white solid with the yield of 70%. ^{1}H NMR (400 MHz, chloroform-*d*) δ 8.34 (s, 1H), 8.01 (s, 2H), 7.60 (s, 1H), 6.79 (d, J = 4.1Hz, 1H), 6.28 (d, J = 17.8 Hz, 3H), 3.74 (s, 6H), 3.21 (t, J = 7.7 Hz, 2H), 3.03 (t, J = 7.4 Hz, 2H), NH is missing. LC–MS (ESI): *m/z* 414.20 $[M+H]^+$. HPLC purity: >95%, retention time = 2.995 min. HR-MS *m/z* (ESI) Found 414.1240 $[M+H]^+$, $C_{19}H_{20}N_5O_4S^+$ Calcd. for 414.1231. Compounds **11**, **13**, **17**, **20**, **21** and intermediate **42** were prepared with a similar procedure as used for **12** (see Scheme 1 and Supporting Information Section 5).

4.2.8. *3-((3-(3,5-Dimethoxyphenethyl)-5H-pyrrolo[2,3-b]pyrazin-5-yl)sulfonyl)aniline (**43**)*

3-(3,5-Dimethoxyphenethyl)-5-((3-nitrophenyl)sulfonyl)-5*H*-pyrrolo[2,3-*b*]pyrazine (**42**, 200 mg, 0.5 mmol) was dissolved in methylbenzene. Concentrated hydrochloric acid (1 mL) and Fe powder (168 mg, 3.0 mmol) were added. After the reaction mixture was stirred and refluxed for 30 min. After the reaction finished (monitored by TLC), the resulting solution was filtered and filtrate was concentrated under reduced pressure. Then saturated $NaHCO_3$ solution was added and extracted with ethyl acetate. The organic layer was washed with brine and dried with Na_2SO_4. The organic phase was concentrated under reduced pressure. The residue was purified by flash chromatography to afford **43** as yellow solid with the yield of 70%. ^{1}H NMR (400 MHz, chloroform-*d*) δ 8.31 (s, 1H), 7.94 (d, J = 4.1Hz, 1H), 7.55 (d, J = 7.9 Hz, 1H), 7.50 (t, J = 2.1Hz, 1H), 7.25 (d, J = 8.0 Hz, 1H), 6.88–6.81 (m, 1H), 6.80 (d, J = 4.2 Hz, 1H), 6.33 (d, J = 1.7 Hz, 3H), 3.92 (s, 2H), 3.75 (s, 6H), 3.30–3.20 (m, 2H), 3.13–3.04 (m, 2H).

4.2.9. *N-(3-((3-(3,5-Dimethoxyphenethyl)-5H-pyrrolo[2,3-b]pyrazin-5-yl)sulfonyl)phenyl)acetamide (**15**)*

3-((3-(3,5-Dimethoxyphenethyl)-5*H*-pyrrolo[2,3-*b*]pyrazin-5-yl)sulfonyl)aniline (**43**, 50 mg, 0.11 mmol), DMAP (1 mg, 0.009 mmol) and DIPEA (28 mg, 0.22 mmol) were dissolved in anhydrous CH_2Cl_2 and the mixture was cooled to 0 °C. Acetyl chloride (9 mg, 0.11 mmol) was slowly added to the above solution. Then the mixture was stirred for 15 min at room temperature. Then saturated $NaHCO_3$ solution was added and the organic layer was washed with brine and dried with Na_2SO_4. The organic phase was concentrated under reduced pressure. The residue was purified by flash chromatography to afford **15** as white solid with the yield of 73%. ^{1}H NMR (400 MHz, chloroform-*d*) δ 8.29 (d, J = 15.4 Hz, 2H), 7.94–7.86 (m, 3H), 7.63 (s, 1H), 7.43 (t, J = 8.1Hz, 1H), 6.77 (d, J = 4.1Hz, 1H), 6.31 (s, 3H), 3.73 (s, 6H), 3.19 (t, J = 7.8 Hz, 2H), 3.01 (t, J = 7.7 Hz, 2H), 2.07 (s, 3H). LC–MS (ESI): *m/z* 481.24 $[M+H]^+$. HPLC purity: >92%, retention time = 3.435 min. HR-MS *m/z* (ESI) Found 481.1538 $[M+H]^+$, $C_{24}H_{25}N_4O_5S^+$ Calcd. for 481.1540.

4.2.10. *Ethyl2-(4-((3-(3,5-dimethoxyphenethyl)-5H-pyrrolo[2,3-b]pyrazin-5-yl)sulfonyl)-1H-imidazol-1-yl)acetate (**14**)*

Ethyl bromoacetate (44 mg, 0.266 mmol) and K_2CO_3 (67 mg, 0.484 mmol) was added to a solution of 5-((1*H*-imidazol-4-yl)sulfonyl)-3-(3,5-dimethoxyphenethyl)-5*H*-pyrrolo[2,3-*b*]pyrazine (**12**, 100 mg, 0.242 mmol) in DMF, and the reaction mixture was stirred at 60 °C for 2 h. After the reaction finished (monitored by TLC), water was added. The mixture was extracted three times with CH_2Cl_2, washed with brine and dried with Na_2SO_4. The organic phase was concentrated under reduced pressure. The residue was purified by flash chromatography to afford **14** as white solid with the yield of 74%. ^{1}H NMR (400 MHz, chloroform-*d*) δ 8.34 (s, 1H), 8.05 (d, J = 4.1Hz, 1H), 8.01 (d, J = 1.4 Hz, 1H), 7.45 (d, J = 1.4 Hz, 1H), 6.81 (d, J = 4.1Hz, 1H), 6.34–6.29 (m, 3H), 4.72 (s, 2H), 3.75 (s, 6H), 3.50 (q, J = 7.0 Hz, 2H), 3.21 (dd, J = 9.0, 6.5 Hz, 2H), 3.03 (dd, J = 8.9, 6.5 Hz, 2H), 1.23 (t, J = 7.0 Hz, 3H). LC–MS (ESI): *m/z* 500.10 $[M+H]^+$. Compounds **22**–**28** were prepared with a similar procedure as used for **14** (see Scheme 1 and Supporting Information).

4.2.11. *3-(3,5-Dimethoxyphenethyl)-5-(phenylsulfonyl)-5H-pyrrolo[2,3-b]pyrazine (**5**)*

3-(3,5-Dimethoxyphenethyl)-5*H*-pyrrolo[2,3-*b*]pyrazine (**41**, 1 g, 3.5 mmol) and NaH (93 mg, 3.85 mmol) were dissolved in anhydrous DMF. After the reaction mixture was stirred at 0 °C for 10 min. Benzenesulfonyl chloride (680 mg, 3.85 mmol) in anhydrous DMF was slowly added in drops, and the mixture was stirred for 20 min at room temperature. Then the resulting solution was poured into H_2O and extracted with CH_2Cl_2. The organic layer was washed with brine and dried with Na_2SO_4.

The organic phase was concentrated under reduced pressure. The residue was purified by flash chromatography to afford **5** as white solid with the yield of 73%. ^{1}H NMR (400 MHz, chloroform-*d*) δ 8.32 (s, 1H), 8.28–8.23 (m, 2H), 7.97 (d, J = 4.1Hz, 1H), 7.67–7.59 (m, 1H), 7.53 (t, J = 7.8 Hz, 2H), 6.81 (d, J = 4.2 Hz, 1H), 6.33 (s, 3H), 3.76 (s, 6H), 3.24 (dd, J = 9.0, 6.5 Hz, 2H), 3.07 (dd, J = 9.0, 6.6 Hz, 2H). LC–MS (ESI): *m/z* 424.18 $[M+H]^+$. HPLC purity: >98%, retention time = 3.71 min.

4.2.12. 3-(2,6-Dichloro-3,5-dimethoxyphenethyl)-5-(phenylsulfonyl)-5H-pyrrolo[2,3-b]pyrazine (7)

To a solution of 3-(3,5-dimethoxyphenethyl)-5-(phenylsulfonyl)-5*H*-pyrrolo[2,3-*b*]pyrazine (**5**, 4.34 g, 10.3 mmol) in 150 mL of CH_2Cl_2 at 0 °C, sulfuryl dichloride (2.8 g, 20.6 mmol) was added slowly. After stirring for 30 min at room temperature, saturated $NaHCO_3$ solution was added, and the organic phase was washed with brine (100 mL), and dried over Na_2SO_4. Then the organic phase was concentrated under reduced pressure. The residue was purified by flash chromatography to afford **7** as white solid with the yield of 83%. ^{1}H NMR (400 MHz, chloroform-*d*) δ 8.35 (s, 1H), 8.32 (d, J = 7.4 Hz, 2H), 7.99 (d, J = 4.2 Hz, 1H), 7.63 (t, J = 7.3 Hz, 1H), 7.56 (t, J = 7.7 Hz, 2H), 6.81 (d, J = 4.2 Hz, 1H), 6.54 (s, 1H), 3.96 (s, 6H), 3.39 (dd, J = 9.5, 6.7 Hz, 2H), 3.21–3.12 (m, 2H). LC–MS (ESI): *m/z* 492.14 $[M+H]^+$. HPLC purity: >94%, retention time = 4.175 min. HR-MS *m/z* (ESI) Found 492.0533 $[M+H]^+$, $C_{22}H_{20}Cl_2N_3O_4S^+$ Calcd. for 492.0546.

4.2.13. 3-(2,6-Dichloro-3,5-dimethoxyphenethyl)-5H-pyrrolo[2,3-b]pyrazine (44)

TBAF/THF (6 mL, 6 mmol) was added to a solution of 3-(2,6-dichloro-3,5-dimethoxyphenethyl)-5-(phenylsulfonyl)-5*H*-pyrrolo[2,3-*b*]pyrazine (**7**, 2 g, 4 mmol) in CH_2Cl_2 (50 mL), and the reaction mixture was stirred at room temperature for 1H. After the reaction finished (monitored by TLC), CH_2Cl_2 was added. The organic phase was washed with water, and dried over Na_2SO_4. Then the organic phase was concentrated under reduced pressure. The residue was purified by flash chromatography to afford **44** as gray solid with the yield of 85%. ^{1}H NMR (400 MHz, chloroform-*d*) δ 8.32 (s, 1H), 7.41 (d, J = 3.5 Hz, 1H), 6.65 (d, J = 3.6 Hz, 1H), 6.51 (s, 1H), 3.94 (s, 6H), 3.53–3.42 (m, 2H), 3.22–3.12 (m, 2H), NH is missing.

4.2.14. 3-(2,6-Dichloro-3,5-dimethoxyphenethyl)-5-((2-nitrophenyl)sulfonyl)-5H-pyrrolo[2,3-b]pyrazine (45)

3-(2,6-Dichloro-3,5-dimethoxyphenethyl)-5*H*-pyrrolo[2,3-*b*]pyrazine (**44**, 1 g, 2.85 mmol) and NaH (75 mg, 3.14 mmol) was dissolved in anhydrous DMF. After the reaction mixture was stirred at 0 °C for 10 min. 2-Nitrobenzenesulfonyl chloride (696 mg, 3.14 mmol) in anhydrous DMF was slowly added in drops, and the mixture was stirred for 30 min at room temperature. Then the resulting solution was poured into H_2O and extracted with CH_2Cl_2. The organic layer was washed with brine and dried with Na_2SO_4. The organic phase was concentrated under reduced pressure. The residue was purified by flash chromatography to afford **45** as yellow solid with the yield of 76%. ^{1}H NMR (400 MHz, chloroform-*d*) δ 8.94 (d, J = 7.5 Hz, 1H), 8.43 (s, 1H), 8.00 (d, J = 4.1Hz, 1H), 7.89 (d, J = 7.7 Hz, 1H), 7.81 (t, J = 7.6 Hz, 1H), 7.75 (d, J = 8.4 Hz, 1H), 6.89 (d, J = 3.7 Hz, 1H), 6.55 (s, 1H), 3.97 (s, 6H), 3.44–3.32 (m, 2H), 3.21–3.08 (m, 2H).

4.2.15. Imidazo[1,2-b]pyridazine-3-sulfonic acid (68)

Imidazo[1,2-*b*]pyridazine (**67**, 1.5 g, 12.6 mmol) was dissolved in $CHCl_3$. Chlorosulfonic acid (2.35 mL) dissolved in 10 mL $CHCl_3$ was slowly added in drops, and the mixture was stirred for 20 h at 65 °C. The resulting solution was concentrated under reduced pressure. Then EtOH was added and the solution was sonicated. The solid was filtered and dissolved in NaOH solution (1 mol/L). The resulting solution was extracted with CH_2Cl_2. Then 1 mol/L hydrochloric acid was added to the aqueous phase to pH = 2. The solid was filtered and dried to afford **68** as white solid with the yield of 90%. ^{1}H NMR (400 MHz, DMSO-d_6) δ 8.97 (m, 1H), 8.47 (s, 1H), 7.89 (d, J = 9.6 Hz, 1H), 7.83 (dd, J = 9.5, 1.7 Hz, 1H). OH is missing.

4.2.16. Imidazo[1,2-b]pyridazine-3-sulfonyl chloride (69)

Imidazo[1,2-*b*]pyridazine-3-sulfonic acid (**68**, 1 g, 5 mmol) and PCl_5 (104 mg, 0.5 mmol) was dissolved in $POCl_3$. After the reaction mixture was stirred at 110 °C for 8 h. After the reaction finished (monitored by TLC), the reaction mixture was evaporated to dryness. Then CH_2Cl_2 was added. Then the organic layer was washed with ice water and dried with Na_2SO_4. The organic phase was concentrated under reduced pressure. The residue was purified by flash chromatography to afford **69** as white solid with the yield of 54%. ^{1}H NMR (400 MHz, chloroform-*d*) δ 8.77 (dd, J = 4.5, 1.5 Hz, 1H), 8.44 (s, 1H), 8.22 (dd, J = 9.1, 1.8 Hz, 1H), 7.50 (dd, J = 9.5, 4.7 Hz, 1H). Compounds **10**, **18**, **19** and **29** were prepared with a similar procedure as used for **45** (see Scheme 1 and Supporting Information Section 5).

4.2.17. 2-((3-(2,6-Dichloro-3,5-dimethoxyphenethyl)-5H-pyrrolo[2,3-b]pyrazin-5-yl)sulfonyl)aniline (46)

3-(2,6-Dichloro-3,5-dimethoxyphenethyl)-5-((2-nitrophenyl)sulfonyl)-5*H*-pyrrolo[2,3-*b*]pyrazine (**45**, 200 mg, 0.4 mmol) was dissolved in methylbenzene. Concentrated hydrochloric acid (1 mL) and Fe powder (135 mg, 2.4 mmol) were added. After the reaction mixture was stirred and refluxed for 30 min. After the reaction finished (monitored by TLC), the resulting solution was filtered and filtrate was concentrated under reduced pressure. Then saturated $NaHCO_3$ solution was added and extracted with ethyl acetate. The organic layer was washed with brine and dried with Na_2SO_4. The organic phase was concentrated under reduced pressure. The residue was purified by flash chromatography to afford **46** as yellow solid with the yield of 75%. ^{1}H NMR (400 MHz, chloroform-*d*) δ 8.94 (d, J = 7.5 Hz, 1H), 8.43 (s, 1H), 8.00 (d, J = 4.1Hz, 1H), 7.89 (d, J = 7.7 Hz, 1H), 7.81 (t, J = 7.6 Hz, 1H), 7.75 (d, J = 8.4 Hz, 1H), 6.89 (d, J = 3.7 Hz, 1H), 6.55 (s, 1H), 5.24 (s, 2H), 3.97 (s, 6H), 3.44–3.32 (m, 2H), 3.21–3.08 (m, 2H).

4.2.18. N-(2-((3-(2,6-dichloro-3,5-dimethoxyphenethyl)-5H-pyrrolo[2,3-b]pyrazin-5-yl)sulfonyl)phenyl)acetamide (16)

2-((3-(2,6-Dichloro-3,5-dimethoxyphenethyl)-5*H*-pyrrolo[2,3-*b*]pyrazin-5-yl)sulfonyl)aniline (**46**, 50 mg, 0.09 mmol), DMAP (1 mg, 0.0072 mmol) and DIPEA (24 mg, 0.18 mmol) were dissolved in anhydrous CH_2Cl_2 and the mixture was cooled to 0 °C. Acetyl chloride (7 mg, 0.09 mmol) was slowly added to the above solution. Then the mixture was stirred for 15 min at room temperature. Then saturated $NaHCO_3$ solution was added and the organic layer was washed with brine and dried with Na_2SO_4. The organic phase was concentrated under reduced pressure. The residue was purified by flash chromatography to afford **16** as

white solid with the yield of 74%. ^{1}H NMR (400 MHz, chloroform-*d*) δ 9.82 (s, 1H), 8.40 (d, J = 8.3 Hz, 1H), 8.31 (s, 1H), 8.13 (dd, J = 8.2, 1.5 Hz, 1H), 7.96 (d, J = 4.1Hz, 1H), 7.66–7.55 (m, 1H), 7.27–7.21 (m, 1H), 6.85 (d, J = 4.1Hz, 1H), 6.50 (s, 1H), 3.93 (s, 6H), 3.34 (dd, J = 9.0, 6.6 Hz, 2H), 3.15 (dd, J = 9.0, 6.7 Hz, 2H), 2.35 (s, 3H). LC–MS (ESI): *m/z* 548.97 $[M+H]^+$. HPLC purity: >96%, retention time = 3.68 min. HR-MS *m/z* (ESI) Found 549.0757 $[M+H]^+$, $C_{24}H_{23}Cl_2N_4O_5S^+$ Calcd. for 549.0761.

*4.2.19. ((3,5-Dimethoxyphenyl)ethynyl)trimethylsilane (**48**)*

1-Bromo-3,5-dimethoxybenzene (**47**, 1 g, 4.6 mmol), TMSA (497 mg, 5.06 mmol), $Pd(PPh_3)_2Cl_2$ (26 mg, 0.23 mmol), CuI (44 mg, 0.23 mmol) and triethylamine (931 mg, 9.2 mmol) were dissolved in DMF and the resultant solution was purged with argon. The reaction mixture was stirred at 100 °C for 3 h. The reaction mixture was allowed to cool to room temperature and concentrated to dryness under vacuum. The residue was purified by flash chromatography to afford **48** as yellow solid with the yield of 84%. ^{1}H NMR (400 MHz, chloroform-*d*) δ 6.64 (d, J = 2.2 Hz, 2H), 6.46 (t, J = 2.3 Hz, 1H), 3.80 (s, 6H), 0.27 (s, 9H).

*4.2.20. ((2,6-Dichloro-3,5-dimethoxyphenyl)ethynyl) trimethylsilane (**49**)*

To a solution of ((3,5-dimethoxyphenyl)ethynyl)trimethylsilane (**48**, 900 mg, 3.8 mmol) in CH_2Cl_2 at 0 °C, sulfuryl dichloride (1 g, 7.4 mmol) was added slowly. After stirring for 30 min at room temperature, saturated $NaHCO_3$ solution was added, and the organic phase was washed with brine, and dried over Na_2SO_4. Then the organic phase was concentrated under reduced pressure. The residue was purified by flash chromatography to afford **49** as gray solid with the yield of 80%. ^{1}H NMR (400 MHz, chloroform-*d*) δ 6.48 (s, 1H), 3.80 (s, 6H), 0.27 (s, 9H).

*4.2.21. 2,4-Dichloro-3-ethynyl-1,5-dimethoxybenzene (**50**)*

TBAF/THF (2.9 ml, 2.9 mmol) was added to a solution of ((2,6-dichloro-3,5-dimethoxyphenyl)ethynyl)trimethylsilane (**49**, 800 mg, 2.6 mmol) in CH_2Cl_2, and the reaction mixture was stirred at room temperature for 1H. After the reaction finished (monitored by TLC), CH_2Cl_2 was added. The organic phase was washed with water, and dried over Na_2SO_4. Then the organic phase was concentrated under reduced pressure. The residue was purified by flash chromatography to afford **50** as white solid with the yield of 88%. ^{1}H NMR (400 MHz, chloroform-*d*) δ 6.48 (s, 1H), 3.80 (s, 6H), 3.07 (s, 1H).

*4.2.22. 3-((2,6-Dichloro-3,5-dimethoxyphenyl)ethynyl)-5-(phenylsulfonyl)-5H-pyrrolo[2,3-b]pyrazine (**9**)*

A solution of 3-bromo-5-(phenylsulfonyl)-5*H*-pyrrolo[2,3-*b*]pyrazine (**39,** 100 mg, 0.3 mmol), 2,4-dichloro-3-ethynyl-1,5-dimethoxybenzene (**50**, 76 mg, 0.33 mmol), $Pd(PPh_3)_2Cl_2$ (35 mg, 0.03 mmol), CuI (6 mg, 0.03 mmol) and triethylamine (61 mg, 0.6 mmol) in DMF in a microwave tube was flushed with N_2 for 5 min then sealed. The tube was heated at 100 °C for 3 h. Then the reaction mixture was evaporated to dryness. The residue was purified by flash chromatography to give **9** as gray solid with the yield of 83%. ^{1}H NMR (400 MHz, chloroform-*d*) δ 8.77 (s, 1H), 8.32 (d, J = 7.9 Hz, 2H), 8.10 (d, J = 4.1Hz, 1H), 7.64 (t, J = 7.4 Hz, 1H), 7.56 (t, J = 7.7 Hz, 2H), 6.86 (d, J = 4.1Hz, 1H), 6.65 (s, 1H), 3.99 (s, 6H). LC–MS (ESI): *m/z* 488.10 $[M+H]^+$. HPLC purity: >93%, retention time = 4.12 min.

*4.2.23. 2,6-Dichloro-3,5-dimethoxybenzaldehyde (**52**)*

To a solution of 3,5-dimethoxybenzaldehyde (**51**, 300 mg, 1.8 mmol) in 50 mL of CH_2Cl_2 at 0 °C, sulfuryl dichloride (486 mg, 3.6 mmol) was added slowly. After stirring for 30 min at room temperature, saturated $NaHCO_3$ solution was added, and the organic phase was washed with brine, and dried over Na_2SO_4. Then the organic phase was concentrated under reduced pressure. The residue was purified by flash chromatography to afford **52** as white solid with the yield of 80%. ^{1}H NMR (400 MHz, chloroform-*d*) δ 10.47 (s, 1H), 6.73 (s, 1H), 3.98 (s, 6H).

*4.2.24. 2,4-Dichloro-1,5-dimethoxy-3-vinylbenzene (**53**)*

Methyltriphenylphosphonium bromide (512 mg, 1.43 mmol) was dissolved in dry THF and the solution was degassed by argon. After the solution was cooled to −10 °C, potassium *t*-butoxide (160 mg, 1.43 mmol) was added. The resulting mixture was stirred at −10 °C for 1H. Then a solution of 2,6-dichloro-3,5-dimethoxybenzaldehyde (**52,** 300 mg, 1.3 mmol) in dry THF was slowly added to the above mixture at 0 °C. The mixture was stirred for 8 h at room temperature. Then the resulting solution was poured into H_2O and extracted with ethyl acetate. The organic layer was washed with brine and dried with Na_2SO_4. The organic phase was concentrated under reduced pressure. The residue was purified by flash chromatography to afford **53** as white solid with the yield of 76%. ^{1}H NMR (400 MHz, chloroform-*d*) δ 7.33 (s, 1H), 6.68 (dd, J = 17.7, 11.8 Hz, 1H), 6.50 (d, J = 8.8 Hz, 1H), 5.71 (d, J = 9.2 Hz, 1H), 3.91 (s, 6H).

*4.2.25. (E)-3-(2,6-Dichloro-3,5-dimethoxystyryl)-5-(phenylsulfonyl)-5H-pyrrolo[2,3-b]pyrazine (**8**)*

A solution of 3-bromo-5-(phenylsulfonyl)-5*H*-pyrrolo[2,3-*b*]pyrazine (**39**, 100 mg, 0.3 mmol), 2,4-dichloro-1,5-dimethoxy-3-vinylbenzene (**53**, 84 mg, 0.36 mmol), $Pd(OAc)_2$ (4 mg, 0.015 mmol), PPh_3 (4 mg, 0.015 mmol) and triethylamine (67 mg, 0.66 mmol) in CH_3CN in a microwave tube was flushed with N_2 for 5 min then sealed. The tube was heated at 85 °C for 3 h. Then the reaction mixture was evaporated to dryness. The residue was purified by flash chromatography to give **8** as white solid with the yield of 73%. ^{1}H NMR (400 MHz, chloroform-*d*) δ 8.51 (s, 1H), 8.34–8.28 (m, 2H), 8.03 (d, J = 4.3 Hz, 1H), 7.97 (d, J = 16.2 Hz, 1H), 7.61 (t, J = 7.5 Hz, 1H), 7.54 (t, J = 7.6 Hz, 2H), 7.32 (s, 1H), 6.81 (d, J = 4.1Hz, 1H), 6.59 (s, 1H), 3.97 (s, 6H). LC–MS (ESI): *m/z* 490.10 $[M+H]^+$. HPLC purity: >93%, retention time = 3.89 min.

*4.2.26. 3-((3-Ethoxyphenyl)ethynyl)-5H-pyrrolo[2,3-b]pyrazine (**54a**)*

A solution of 3-bromo-5*H*-pyrrolo[2,3-*b*]pyrazine (**38,** 100 mg, 0.5 mmol), 1-ethoxy-3-ethynylbenzene (81 mg, 0.55 mmol), $Pd(PPh_3)_2Cl_2$ (29 mg, 0.025 mmol), CuI (5 mg, 0.025 mmol) and triethylamine (101 mg, 1 mmol) in DMF in a microwave tube was flushed with N_2 for 5 min then sealed. The tube was heated at 100 °C for 3 h. Then the reaction mixture was evaporated to dryness. The residue was purified by flash chromatography to give **54a** as yellow solid with the yield of 83%. ^{1}H NMR (400 MHz, chloroform-*d*) δ 10.00 (s, 1H), 8.74 (s, 1H), 7.72 (s, 1H), 7.32 (t, J = 7.9 Hz, 1H), 7.25 (d, J = 7.4 Hz, 1H), 7.18 (s, 1H), 6.98

(d, J = 8.1Hz, 1H), 6.81 (s, 1H), 4.09 (q, J = 6.9 Hz, 2H), 1.47 (t, J = 6.9 Hz, 3H). Intermediate **54b** was prepared with a similar procedure as used for **54a** (see Scheme 2 and Supporting Information Section 5).

*4.2.27. 3-(3-Ethoxyphenethyl)-5H-pyrrolo[2,3-b]pyrazine (**55a**)*
Hydrogen gas was applied (2 bar) onto a solution of 3-((3-ethoxyphenyl)ethynyl)-5*H*-pyrrolo[2,3-*b*]pyrazine (**54a**, 100 mg) and dry Pd–C (10 mg) in EtOH. Then the mixture was stirred for 4 h at 30 °C. After the reaction finished (monitored by TLC), the solid was separated by decantation and filtration. The liquid was concentrated under reduced pressure. The crude mixture was purified by flash column chromatography on silica gel to afford compound **55a** as white solid with the yield of 82%. ^{1}H NMR (400 MHz, chloroform-*d*) δ 9.96 (s, 1H), 8.36 (s, 1H), 7.57 (t, J = 3.2 Hz, 1H), 7.21 (t, J = 7.8 Hz, 1H), 6.84–6.71 (m, 4H), 4.01 (q, J = 7.0 Hz, 2H), 3.25 (dd, J = 9.7, 6.3 Hz, 2H), 3.12 (dd, J = 9.5, 6.5 Hz, 2H), 1.41 (t, J = 7.0 Hz, 3H). Intermediate **55b** was prepared with a similar procedure as used for **55a** (see Scheme 2 and Supporting Information).

*4.2.28. 3-(3-Ethoxyphenethyl)-5-((1-methyl-1H-imidazol-4-yl) sulfonyl)-5H-pyrrolo[2,3-b]pyrazine (**30**)*
3-(3-Ethoxyphenethyl)-5*H*-pyrrolo[2,3-*b*]pyrazine (**55a**, 50 mg, 0.19 mmol) and NaH (5 mg, 0.21 mmol) were dissolved in anhydrous DMF. After the reaction mixture was stirred at 0 °C for 10 min. 1-Methyl-1*H*-imidazole-4-sulfonyl chloride (38 mg, 0.21 mmol) in anhydrous DMF was slowly added in drops, and the mixture was stirred for 30 min at room temperature. Then the resulting solution was poured into H_2O and extracted with CH_2Cl_2. The organic layer was washed with brine and dried with Na_2SO_4. The organic phase was concentrated under reduced pressure. The residue was purified by flash chromatography to afford **30** as white solid with the yield of 76%. ^{1}H NMR (400 MHz, chloroform-*d*) δ 8.28 (s, 1H), 8.03 (d, J = 4.2 Hz, 1H), 7.93–7.85 (m, 1H), 7.46–7.37 (m, 1H), 7.14 (t, J = 7.8 Hz, 1H), 6.79 (d, J = 4.2 Hz, 1H), 6.71 (dd, J = 8.1, 2.0 Hz, 1H), 6.68–6.60 (m, 2H), 3.95 (q, J = 7.0 Hz, 2H), 3.67 (s, 3H), 3.20 (t, J = 7.6 Hz, 2H), 3.05 (t, J = 7.6 Hz, 2H), 1.37 (t, J = 7.0 Hz, 3H). LC–MS (ESI): *m/z* 412.10 $[M+H]^+$. HPLC purity: >98%, retention time = 3.304 min. HR-MS *m/z* (ESI) Found 412.1444 $[M+H]^+$, $C_{20}H_{22}N_5O_3S^+$ Calcd. for 412.1438. Compound **31** was prepared with a similar procedure as used for **30** (see Scheme 2 and Supporting Information).

*4.2.29. 1-Ethynyl-3,5-dimethoxybenzene (**56**)*
TBAF/THF (2.2 mL, 2.2 mmol) was added to a solution of ((3,5-dimethoxyphenyl)ethynyl)trimethylsilane (**48**, 500 mg, 2 mmol) in CH_2Cl_2, and the reaction mixture was stirred at room temperature for 1H. After the reaction finished (monitored by TLC), CH_2Cl_2 was added. The organic phase was washed with water, and dried over Na_2SO_4. Then the organic phase was concentrated under reduced pressure. The residue was purified by flash chromatography to afford **56** as white solid with the yield of 78%. ^{1}H NMR (400 MHz, chloroform-*d*) δ 6.67 (d, J = 2.3 Hz, 2H), 6.49 (t, J = 2.3 Hz, 1H), 3.81 (s, 6H), 3.07 (s, 1H).

*4.2.30. 1-Ethynyl-2-fluoro-3,5-dimethoxybenzene (**57**)*
To a solution of 1-ethynyl-3,5-dimethoxybenzene (**56**, 300 mg, 1.85 mmol) in CH_2Cl_2 at 0 °C, selectflour (709 mg, 2 mmol) was added slowly. After stirring for 20 h at room temperature, the solution was concentrated under reduced pressure and CH_2Cl_2 was added. Then saturated $NaHCO_3$ solution was added, and the organic phase was washed with brine (100 mL), and dried over Na_2SO_4. Then the organic phase was concentrated under reduced pressure. The residue was purified by flash chromatography to afford **57** as white solid with the yield of 50%. ^{1}H NMR (400 MHz, chloroform-*d*) δ 6.56 (dd, J = 7.0, 2.9 Hz, 1H), 6.53–6.49 (m, 1H), 3.88 (s, 3H), 3.79 (s, 3H), 3.32 (s, 1H). Intermediate **58** was prepared with a similar procedure as used for **57** (see Scheme 3 and Supporting Information Section 5).

*4.2.31. 3-((2-Fluoro-3,5-dimethoxyphenyl)ethynyl)-5H-pyrrolo [2,3-b]pyrazine (**59**)*
A solution of 3-bromo-5*H*-pyrrolo[2,3-*b*]pyrazine (**38,** 100 mg, 0.5 mmol), 1-ethynyl-2-fluoro-3,5-dimethoxybenzene (**57**, 100 mg, 0.55 mol), $Pd(PPh_3)_2Cl_2$ (29 mg, 0.025 mmol), CuI (5 mg, 0.025 mmol) and triethylamine (101 mg, 1 mmol) in DMF in a microwave tube was flushed with N_2 for 5 min then sealed. The tube was heated at 90 °C for 8 h. Then the reaction mixture was evaporated to dryness. The residue was purified by flash chromatography to give **59** as yellow solid with the yield of 84%. ^{1}H NMR (400 MHz, DMSO-d_6) δ 12.26 (s, 1H), 8.64 (s, 1H), 8.06 (t, J = 3.1Hz, 1H), 6.86 (dd, J = 7.3, 2.8 Hz, 1H), 6.77 (d, J = 4.5 Hz, 1H), 6.72 (s, 1H), 3.88 (s, 3H), 3.81 (s, 3H).

*4.2.32. 3-(2-Fluoro-3,5-dimethoxyphenethyl)-5H-pyrrolo[2,3-b] pyrazine (**60**)*
A solution of 3-((2-fluoro-3,5-dimethoxyphenyl)ethynyl)-5*H*-pyrrolo[2,3-*b*]pyrazine (**59**, 80 mg) in EtOH, $Pd(OH)_2$ (8 mg) was added. The solution was stirred at 50 °C for 6 h under H_2. After the reaction finished (monitored by TLC), the solution was filtered and evaporated to dryness. The residue was purified by flash chromatography to give **60** as white solid with the yield of 85%. ^{1}H NMR (400 MHz, chloroform-*d*) δ 9.36 (s, 1H), 8.35 (s, 1H), 7.66–7.51 (m, 1H), 6.74 (dd, J = 3.7, 2.0 Hz, 1H), 6.41 (dd, J = 6.7, 2.9 Hz, 1H), 6.23 (dd, J = 4.9, 3.0 Hz, 1H), 3.87 (s, 3H), 3.72 (s, 3H), 3.23 (dd, J = 9.2, 5.5 Hz, 2H), 3.19–3.08 (m, 2H).

*4.2.33. 3-(2-Fluoro-3,5-dimethoxyphenethyl)-5-((1-methyl-1H-imidazol-4-yl)sulfonyl)-5H-pyrrolo[2,3-b]pyrazine (**32**)*
3-(2-Fluoro-3,5-dimethoxyphenethyl)-5*H*-pyrrolo[2,3-*b*]pyrazine (**60**, 50 mg, 0.17 mmol) and NaH (5 mg, 0.19 mmol) was dissolved in anhydrous DMF. After the reaction mixture was stirred at 0 °C for 10 min. 1-Methyl-1*H*-imidazole-4-sulfonyl chloride (34 mg, 0.19 mmol) in 5 mL of anhydrous DMF was slowly added in drops, and the mixture was stirred for 30 min at room temperature. Then the resulting solution was poured into H_2O and extracted with CH_2Cl_2. The organic layer was washed with brine and dried with Na_2SO_4. The organic phase was concentrated under reduced pressure. The residue was purified by flash chromatography to afford **32** as white solid with the yield of 77%. ^{1}H NMR (400 MHz, chloroform-*d*) δ 8.33 (s, 1H), 8.06 (d, J = 4.1Hz, 1H), 8.00 (s, 1H), 7.43 (s, 1H), 6.81 (d, J = 4.2 Hz, 1H), 6.41 (dd, J = 6.8, 3.0 Hz, 1H), 6.24–6.18 (m, 1H), 3.87 (s, 3H), 3.77 (s, 3H), 3.74 (s, 3H), 3.28–3.16 (m, 2H), 3.14–3.05 (m, 2H). LC–MS (ESI): *m/z* 446.18 $[M+H]^+$. HPLC purity: >96%, retention time = 3.08 min. HR-MS *m/z* (ESI) Found 446.1304 $[M+H]^+$, $C_{20}H_{21}FN_5O_4S^+$ Calcd. for 446.1293.

*4.2.34. 3-Bromo-5-((1-methyl-1H-imidazol-4-yl)sulfonyl)-5H-pyrrolo[2,3-b]pyrazine (**61**)*

3-Bromo-5*H*-pyrrolo[2,3-*b*]pyrazine (**38,** 100 mg, 0.5 mmol) and NaH (13 mg, 0.55 mmol) was dissolved in anhydrous DMF. After the reaction mixture was stirred at 0 °C for 10 min. 1-Methyl-1*H*-imidazole-4-sulfonyl chloride (99 mg, 0.55 mmol) in 5 mL of anhydrous DMF was slowly added in drops, and the mixture was stirred for 30 min at room temperature. Then the resulting solution was poured into H_2O and extracted with CH_2Cl_2. The organic layer was washed with brine and dried with Na_2SO_4. The organic phase was concentrated under reduced pressure. The residue was purified by flash chromatography to afford **61** as white solid with the yield of 80%. ^{1}H NMR (400 MHz, DMSO-d_6) δ 8.76 (s, 1H), 8.38 (d, J = 1.3 Hz, 1H), 8.24 (d, J = 4.1Hz, 1H), 7.82 (d, J = 1.1Hz, 1H), 7.04 (d, J = 4.2 Hz, 1H), 3.71 (s, 3H).

*4.2.35. 3-((2,6-Difluoro-3,5-dimethoxyphenyl)ethynyl)-5-((1-methyl-1H-imidazol-4-yl)sulfonyl)-5H-pyrrolo[2,3-b]pyrazine (**62**)*

A solution of 3-bromo-5-((1-methyl-1*H*-imidazol-4-yl)sulfonyl)-5*H*-pyrrolo[2,3-*b*]pyrazine (**61,** 80 mg, 0.24 mmol), 3-ethynyl-2,4-difluoro-1,5-dimethoxybenzene (**58**, 80 mg, 0.23 mmol), $Pd(PPh_3)_2Cl_2$ (14 mg, 0.012 mmol), CuI (3 mg, 0.012 mmol) and triethylamine (47 mg, 0.46 mmol) in DMF in a microwave tube was flushed with N_2 for 5 min then sealed. The tube was heated at 90 °C for 8 h. Then the reaction mixture was evaporated to dryness. The residue was purified by flash chromatography to give **62** as yellow solid with the yield of 79%. ^{1}H NMR (400 MHz, DMSO-d_6) δ 8.84 (s, 1H), 8.37 (d, J = 4.1Hz, 2H), 7.81 (s, 1H), 7.21 (t, J = 8.4 Hz, 1H), 7.08 (d, J = 4.1Hz, 1H), 3.93 (s, 6H), 3.70 (s, 3H).

*4.2.36. (E)-3-(2,6-Difluoro-3,5-dimethoxystyryl)-5-((1-methyl-1H-imidazol-4-yl)sulfonyl)-5H-pyrrolo[2,3-b]pyrazine (**34**)*

A solution of 3-((2,6-difluoro-3,5-dimethoxyphenyl)ethynyl)-5-((1-methyl-1*H*-imidazol-4-yl)sulfonyl)-5*H*-pyrrolo[2,3-*b*]pyrazine (**62**, 50 mg) in EtOH, $Pd(OH)_2$ (10 mg) was added. The solution was stirred at 50 °C for 6 h under H_2. After the reaction finished (monitored by TLC), the solution was filtered and evaporated to dryness. The residue was purified by flash chromatography to give **34** as yellow solid with the yield of 75%. ^{1}H NMR (400 MHz, DMSO-d_6) δ 8.46 (s, 1H), 8.18 (d, J = 4.1Hz, 1H), 7.74 (s, 1H), 7.42 (s, 1H), 7.05 (dd, J = 10.2, 5.4 Hz, 2H), 6.93 (t, J = 3.6 Hz, 1H), 6.69 (d, J = 12.6 Hz, 1H), 3.87 (s, 6H), 3.65 (s, 3H). LC–MS (ESI): *m/z* 462.20 $[M+H]^+$. HPLC purity: >95%, retention time = 3.03 min. HR-MS *m/z* (ESI) Found 462.1051 $[M+H]^+$, $C_{20}H_{18}F_2N_5O_4S^+$ Calcd. for 462.1042.

*4.2.37. 5-((1H-Iimidazol-4-yl)sulfonyl)-3-bromo-5H-pyrrolo[2,3-b]pyrazine (**63**)*

3-Bromo-5*H*-pyrrolo[2,3-*b*]pyrazine (**38,** 500 mg, 2.54 mmol) and NaH (67 mg, 2.80 mmol) was dissolved in anhydrous DMF. After the reaction mixture was stirred at 0 °C for 10 min. 1*H*-Imidazole-4-sulfonyl chloride (465 mg, 2.80 mmol) in 5 mL of anhydrous DMF was slowly added in drops, and the mixture was stirred for 30 min at room temperature. Then the resulting solution was poured into H_2O and extracted with CH_2Cl_2. The organic layer was washed with brine and dried with Na_2SO_4. The organic phase was concentrated under reduced pressure. The residue was purified by flash chromatography to afford **63** as white solid with the yield of 80%. ^{1}H NMR (400 MHz, DMSO-d_6) δ 13.29 (s, 1H), 8.75 (s, 1H), 8.36 (d, J = 1.0 Hz, 1H), 8.25 (d, J = 4.1Hz, 1H), 7.86 (d, J = 1.0 Hz, 1H), 7.03 (d, J = 4.0 Hz, 1H).

*4.2.38. 3-Bromo-5-((1-(2-fluoroethyl)-1H-imidazol-4-yl)sulfonyl)-5H-pyrrolo[2,3-b]pyrazine (**64**)*

A solution of 5-((1*H*-imidazol-4-yl)sulfonyl)-3-bromo-5*H*-pyrrolo[2,3-*b*]pyrazine (**63**, 300 mg, 0.92 mmol) in CH_2Cl_2, K_2CO_3 (254 mg, 1.84 mmol) and 1-fluoro-2-iodoethane (176 mg, 1.01 mmol) were added. Then the reaction mixture was stirred at 60 °C for 3 h. After the reaction finished (monitored by TLC), the resulting solution was poured into H_2O and extracted with CH_2Cl_2. The organic layer was washed with brine and dried with Na_2SO_4. The organic phase was concentrated under reduced pressure. The residue was purified by flash chromatography to afford **64** as white solid with the yield of 78%. ^{1}H NMR (400 MHz, chloroform-*d*) δ 8.59 (d, J = 3.1Hz, 1H), 8.18 (s, 1H), 8.12–8.06 (m, 1H), 7.56 (s, 1H), 6.85 (t, J = 3.6 Hz, 1H), 4.74 (dd, J = 46.6, 3.2 Hz, 2H), 4.36 (dd, J = 26.7, 3.7 Hz, 2H).

*4.2.39. 3-((2-Fluoro-3,5-dimethoxyphenyl)ethynyl)-5-((1-(2-fluoroethyl)-1H-imidazol-4-yl)sulfonyl)-5H-pyrrolo[2,3-b]pyrazine (**65**)*

A solution of 3-bromo-5-((1-(2-fluoroethyl)-1*H*-imidazol-4-yl)sulfonyl)-5*H*-pyrrolo[2,3-*b*]pyrazine (**64**, 100 mg, 0.27 mmol), 1-ethynyl-2-fluoro-3,5-dimethoxybenzene (**57**, 54 mg, 0.30 mmol), $Pd(PPh_3)_2Cl_2$ (16 mg, 0.014 mmol), CuI (3 mg, 0.014 mmol) and triethylamine (61 mg, 0.60 mmol) in DMF in a microwave tube was flushed with N_2 for 5 min then sealed. The tube was heated at 90 °C for 8 h. Then the reaction mixture was evaporated to dryness. The residue was purified by flash chromatography to give **65** as yellow solid with the yield of 76%. ^{1}H NMR (400 MHz, DMSO-d_6) δ 8.84 (s, 1H), 8.49 (s, 1H), 8.36 (d, J = 4.1Hz, 1H), 7.89 (s, 1H), 7.08 (d, J = 4.3 Hz, 1H), 6.90 (dd, J = 7.0, 3.0 Hz, 1H), 6.80 (d, J = 4.4 Hz, 1H), 4.72 (dd, J = 47.0, 4.5 Hz, 2H), 4.40 (dd, J = 27.6, 4.5 Hz, 2H), 3.88 (s, 3H), 3.81 (s, 3H). Intermediate **66** was prepared with a similar procedure as used for **65** (see Scheme 3 and Supporting Information).

*4.2.40. 3-(2-Fluoro-3,5-dimethoxyphenethyl)-5-((1-(2-fluoroethyl)-1H-imidazol-4-yl)sulfonyl)-5H-pyrrolo[2,3-b]pyrazine (**33**)*

A solution of 3-((2-fluoro-3,5-dimethoxyphenyl)ethynyl)-5-((1-(2-fluoroethyl)-1*H*-imidazol-4-yl)sulfonyl)-5*H*-pyrrolo[2,3-*b*]pyrazine (**65**, 50 mg) in EtOH, $Pd(OH)_2$ (5 mg) was added. The solution was stirred at 50 °C for 6 h under H_2. After the reaction finished (monitored by TLC), the solution was filtered and evaporated to dryness. The residue was purified by flash chromatography to give **33** as white solid with the yield of 77%. ^{1}H NMR (400 MHz, chloroform-*d*) δ 8.33 (s, 1H), 8.11 (s, 1H), 8.06 (d, J = 4.2 Hz, 1H), 7.54 (s, 1H), 6.82 (d, J = 4.1Hz, 1H), 6.41 (dd, J = 6.9, 2.9 Hz, 1H), 6.20 (dd, J = 5.1, 2.9 Hz, 1H), 4.69 (dt, J = 46.7, 4.5 Hz, 2H), 4.31 (dt, J = 27.2, 4.4 Hz, 2H), 3.86 (s, 3H), 3.73 (s, 3H), 3.19 (dd, J = 8.8, 6.0 Hz, 2H), 3.14–3.00 (m, 2H). LC–MS (ESI): *m/z* 478.10 $[M+H]^+$. HPLC purity: >99%, retention time = 2.96 min. HR-MS *m/z* (ESI) Found 478.1364 $[M+H]^+$, $C_{21}H_{22}F_2N_5O_4S^+$ Calcd. for 478.1355. Compound **35** was prepared with a similar procedure as used for **33** (see Scheme 3 and Supporting Information).

4.3. Protein expression, purification and X-ray crystallography

Human FGFR2-(461–768) A628T and E767Q mutation construct was cloned into a modified pET21b vector (Novagen, Malaysia) between BamHI and XhoI, which places expression under the control of the T7-lacO promoter. The protein was expressed in *Escherichia coli* BL21-Gold(DE3) cells (Stratagene, USA) as an N-terminal fusion to a hexahistidine affinity tag with integrated TEV protease site. A single colony was inoculated in Luria–Bertani media containing 100 μg/mL ampicillin at 37 °C, 250 rpm until the A600 reached 0.3. The culture was then transferred to 18 °C, 250 rpm until the A600 reached 0.6–0.8. Isopropyl 1-thio-β-D-galactopyranoside was added to a final concentration of 0.3 mmol/L, and expression was continued at 18 °C, 160 rpm overnight. Cells were collected by centrifugation, and the pellet was resuspended in lysis buffer (50 mmol/L Hepes, 200 mmol/L NaCl, 5% glycerol, 5 mmol/L B-ME, pH 7.5) and sonicated to open the cells. Supernatant was separated from cell debris by centrifugation at 10,000 × *g* for 40 min at 4 °C and loaded onto a Ni-NTA column (Qiagen, Germany) that equilibrated with the buffer containing 50 mmol/L Hepes, 200 mmol/L NaCl, 5% glycerol, 5 mmol/L B-ME, pH 7.5. The column was washed with 20 column volumes of the buffer containing 50 mmol/L Hepes, 200 mmol/L NaCl, 5% glycerol, 5 mmol/L B-ME and 20 mmol/L imidazole, pH 7.5 and then washed with 20 column volumes of the buffer containing 50 mmol/L Hepes, 200 mmol/L NaCl, 5% glycerol, 5 mmol/L B-ME and 50 mmol/L imidazole, pH 7.5. The target protein was eluted with the buffer containing 50 mmol/L Hepes, 200 mmol/L NaCl, 5% glycerol, 5 mmol/L B-ME and 20 mmol/L imidazole, pH 7.5. The eluted protein was dialyzed in lysis buffer and digested with TEV protease (Invitrogen) to remove the N-terminal His tag at 4 °C overnight. The protein was loaded on a second Ni-NTA column equilibrated with lysis buffer. The untagged protein was eluted by the buffer containing 50 mmol/L Hepes, 200 mmol/L NaCl, 5% glycerol, 5 mmol/L B-ME and 10 mmol/L imidazole, pH 7.5. The purified protein was concentrated and further purified by an S200 column (GE Healthcare, USA) to get 95% purity as assessed by SDS-PAGE analysis stained by Coomassie Brilliant Blue R-250 and concentrated to 10 mg/mL in the 50 mmol/L Tris, 200 mmol/L NaCl, 5% glycerol, 5 mmol/L B-ME pH 7.5.

For crystallization, 10 mg/mL protein was incubated compound for about 3 h and Mcompound:Mprotein is 5:1. The crystals of FGFR2/compound **14** were obtained within 2 days by hanging drop vapor diffusion method at 18 °C. The drop was composed of 1 μL of protein/compound mixture and 1 μL crystallization buffer of 0.2 mol/L ammonium sulfate, 0.1 mol/L MES pH 6.5 and 30% (*w/v*) PEG 5000 MME.

The FGFR2/compound **14** cocrystals were cryo-protected in mother liquor containing 20% glycerol and flash-frozen in liquid nitrogen. Diffraction data were collected at SSRF beamline BL19U1 and processed using HKL3000[25]. The molecular replacement software Phaser was used to solve the structure with a search model from PDB entry 4J95[26]. Iterative structure refinement and model building were performed between Refmac5 and Coot[27,28]. Compounds were observed in the electron density map built into the structure model.

4.4. ELISA kinase assay

The effects of indicated compounds on the activities of FGFR1 kinase (Eurofins, San Francisco, USA) were determined using enzyme-linked immunosorbent assays (ELISAs) with purified recombinant proteins. Briefly, 20 μg/mL poly (Glu, Tyr) 4:1 (Sigma, St Louis, MO, USA) was pre-coated in 96-well plates as a substrate. A 50 μL aliquot of 10 μmol/L ATP solution diluted in kinase reaction buffer (50 mmol/L HEPES [pH 7.4], 50 mmol/L $MgCl_2$, 0.5 mmol/L $MnCl_2$, 0.2 mmol/L Na_3VO_4, and 1 mmol/L DTT) was added to each well; 1 μL of various concentrations of indicated compounds diluted in 1% DMSO (*v/v*) (Sigma, St Louis, MO, USA) were then added to each reaction well. 1% DMSO (*v/v*) was used as the negative control. The kinase reaction was initiated by the addition of purified tyrosine kinase proteins diluted in 49 μL of kinase reaction buffer. After incubation for 60 min at 37 °C, the plate was washed three times with phosphate-buffered saline (PBS) containing 0.1% Tween 20 (T-PBS). Anti-phosphotyrosine (PY99) antibody (Cell Signaling Technology, Danvers, UK) (100 μL, 1:500, diluted in 5 mg/mL BSA T-PBS) was then added. After a 30 min incubation at 37 °C, the plate was washed three times, and 100 μL horseradish peroxidase-conjugated goat anti-mouse IgG (Cell Signaling Technology, Danvers, UK) (1:1000, diluted in 5 mg/mL BSA T-PBS) was added. The plate was then incubated at 37 °C for 30 min and washed 3 times. A 100 μL aliquot of a solution containing 0.03% H_2O_2 and 2 mg/mL *o*-phenylenediamine in 0.1 mol/L citrate buffer (pH 5.5) was added. The reaction was terminated by the addition of 50 μL of 2 mol/L H_2SO_4 as the color changed, and the plate was analyzed using a multi-well spectrophotometer (SpectraMAX190, from Molecular Devices, Palo Alto, CA, USA) at 490 nm. The inhibition rate (%) was calculated using the following equation: $[1-(A_{490}/A_{490\ control})] \times 100$. The IC_{50} values were calculated from the inhibition curves in two separate experiments.

4.5. Cell proliferation assay

Cell proliferation was examined in a FGFR1-translocated KG1 leukemia cell line harboring FGFR1OP-FGFR1 fusion. The original KG1 cell line was purchased from ATCC (CRL-8031) (ATCC, Manassas, USA), and cultured according the ATCC standard protocol. Cells were seeded in 96-well cell culture plates. On the day when seeding, the cells were exposed to various concentrations of compounds and further cultured for 72 h at 37 °C. Cell proliferation was then determined using Cell Counts Kit-8 (CCK8) assay (Dojindo Laboratories, Kumamoto, Japan). The IC_{50} values were calculated by concentration-response curve fitting using the four-parameter method.

4.6. In vitro metabolic stability study

Microsomes (human microsome: Xenotech, Lot No.H0610; Rat microsome: Xenotech, Lot No. R1000 (XenoTech, USA) (0.5 mg/mL) were preincubated with 1 μmol/L of test compound for 5 min at 37 °C in 0.1 mol/L phosphate buffer (pH 7.4) with 1 mmol ethylenediaminetetraacetic acid (EDTA), and 5 mmol $MgCl_2$. The reactions were initiated by adding prewarmed cofactors (1 mmol NADPH). After 0, 5, 10, and 30 min incubation at 37 °C, the reactions were stopped by adding an equal volume of cold acetonitrile. The samples were vortexed for 10 min, and then centrifuged at 10,000 × *g* for 10 min. Supernatants were analyzed by LC–MS/MS for the amount of the remaining parent compound, and the corresponding loss of the parent compound was also determined by LC–MS/MS.

The cytochromes P450 (CYP) enzymatic activities were characterized based on their probe reactions: CYP3A4 (midazolam), CYP2D6 (dextromethorphan), CYP2C9 (diclofenac), CYP1A2

(phenacetin) and CYP2C19 (mephenytoin). Incubation mixtures were prepared in a total volume of 100 μL as follows: 0.2 mg/mL of microsome (human microsome: Xenotech, Lot No. H0610), 1 mmol of NADPH, 100 mmol of phosphate buffer (pH 7.4), probe substrates cocktail (10 μmol/L of midazolam, 100 μmol/L of testosterone, 10 μmol/L of dextromethophan, 20 μmol/L of diclofenac, 100 μmol/L of phenacetin, 100 μmol/L of mephenytoin), and 10 μmol/L of the tested compound or positive control cocktail (10 μmol/L of ketoconazole, 10 μmol/L of quinidine, 100 μmol/L of sulfaphenazole, 10 μmol/L of naphthoflavone, and 1000 μmol/L of tranylcypromine) or negative control (PBS). The final concentration of the organic reagent in the incubation mixtures was less than 1% *v/v*. There was a 5 min preincubation period at 37 °C before the reaction was initiated by adding a nicotinamide adenine dinucleotide phosphate (NADPH)-generating system. Reactions were conducted for 20 min for CYPs. For each probe drug, the percentage of the metabolite conversion was less than 20% of the substrate added. The inhibition rate was calculated as: (the formation of the metabolite of probe substrates with 10 μmol/L of the tested compound)/(the formation of the metabolite of the probe substrates with PBS) × 100%.

4.7. *In vivo pharmacokinetics study*

Compound **35** was subjected to PK studies in CD-1 mice and was administered *via* the oral route at 10 mg/kg. Animal procedures were approved by the Institutional Animal Care and Use Committee at Shanghai Institute of Materia Medica, China. After oral administration, blood samples were collected. 10 μL plasma was precipitated by 100 μL MeOH/CAN (50/50, *v/v*). These samples were mixed on a vortex mixer for 1 min, centrifuged for 5 min at 15,000 rpm (EPPENDORF, Hamburg, Germany), and then 20 μL supernatant liquid was mixed with 20 μL water for 30 s before injection. Linear range is 0.3–10,000 ng/mL.

The analyses were performed on an Acquity ultra performance liquid chromatography (UPLC) system (Waters Corporation, Milford, MA, USA) coupled to a Xevo TQ-S mass spectrometer (Waters Corporation, Milford, MA, USA). Chromatographic separation was performed using an Acquity UPLC BEH C18 (1.7 μm, 50 mm × 2.1 mm, Waters Corporation, Milford, MA, USA) column supplied by Waters at a flow of 0.5 mL/min. Gradient elution were used with a mobile phase composed of solvent A (water containing 0.1% formic acid and 5 mmol/L NH_4AC) and solvent B (acetonitrile containing 0.1% formic acid).

The Xevo TQ-S mass spectrometer was equipped with an electrospray ionization probe and was operated in the positive ion mode. The ionspray voltage was kept at 3000 V at a temperature of 500 °C. The Desolvation gas flow was 1000 L/h. The cone voltages were 42 V. The mass transitions for quantitation were *m/z* 362.112 → *m/z* 115.138 for Wrf-f406 with collision energy 18 V and *m/z* 559.323 → *m/z* 70.131 for compound **35** with collision energy 38 V.

4.8. *In vivo antitumor activity assay*

Female nude mice (4–6 weeks old) were housed and maintained under specific pathogen-free conditions. Animal procedures were approved by the Institutional Animal Care and Use Committee at Shanghai Institute of Materia Medica (China, approval No. 2017-04-DJ-26).The tumor cells at a density of 5×10^6 in 200 μL were injected subcutaneously (s.c.) into the right flank of nude mice and then allowed to grow to 700–800 mm^3, which was defined as a well-developed tumor. Subsequently, the well-developed tumors were cut into 1 mm^3 fragments and transplanted s.c. into the right flank of nude mice using a trocar. When the tumor volume reached 100–150 mm^3, the mice were randomly assigned into a vehicle control group ($n = 12$) and treatment groups ($n = 6$ per group). The control groups were given vehicle alone, and the treatment groups received **35** at the indicated doses *via* oral administration once daily for 3 weeks. The sizes of the tumors were measured twice per week using a microcaliper. Tumor volume (TV) = (length × width^2)/2, and the individual relative tumor volume (RTV) was calculated as follows: $RTV = V_t/V_0$, where V_t is the volume on a particular day and V_0 is the volume at the beginning of the treatment. The RTV was shown on indicated days as the median RTV ± SE indicated for groups of mice. Percent (%) inhibition (TGI) values were measured on the final day of study for the drug-treated mice compared with vehicle-treated mice and were calculated as $100 \times \{1-[(V_{\text{Treated final day}}-V_{\text{Treated day 0}})/(V_{\text{Control final day}}-V_{\text{Control day 0}})]$. Significant differences between the treated versus the control groups ($P \leq 0.05$) were determined using student's *t*-test.

Acknowledgments

We are grateful for financial support from the National Natural Science Foundation of China (Grants No. 81661148046 and 81773762, China) and the "Personalized Medicines—Molecular Signature-based Drug Discovery and Development", Strategic Priority Research Program of the Chinese Academy of Sciences (Grants No. XDA12020317, China), the program for Innovative Research Team of the Ministry of Education (China), and the program for Liaoning Innovative Research Team at Shenyang Pharmaceutical University (China).

Appendix A. Supporting information

Supplementary data associated with this article can be found in the online version at https://doi.org/10.1016/j.apsb.2018.12.008.

References

1. The Cancer Genome Atlas Research Network, Weinstein JN, Collisson EA, Mills GB, Shaw KR, Ozenberger BA, et al. The cancer genome Atlas pan-cancer analysis project. *Nat Genet* 2013;**45**:1113–20.
2. Liu J, Lichtenberg T, Hoadley KA, Poisson LM, Lazar AJ, Cherniack AD, et al. An integrated TCGA pan-cancer clinical data resource to drive high-quality survival outcome analytics. *Cell* 2018;**173**:400–416.e11.
3. Sanchez-Vega F, Mina M, Armenia J, Chatila WK, Luna A, La KC, et al. Oncogenic signaling pathways in the cancer genome atlas. *Cell* 2018;**173**:321–37.e10.
4. Wu P, Nielsen TE, Clausen MH. FDA-approved small-molecule kinase inhibitors. *Trends Pharmacol Sci* 2015;**36**:422–39.
5. Bhullar KS, Lagarón NO, McGowan EM, Parmar I, Jha A, Hubbard BP, et al. Kinase-targeted cancer therapies: progress, challenges and future directions. *Mol Cancer* 2018;**17**:48.
6. Zhao W, Qiu Y, Kong D. Class I phosphatidylinositol 3-kinase inhibitors for cancer therapy. *Acta Pharm Sin B* 2017;**7**:27–37.
7. Harrison PT, Huang PH. Exploiting vulnerabilities in cancer signalling networks to combat targeted therapy resistance. *Essays Biochem* 2018;**62**:583–93.

8. Lategahn J, Keul M, Rauh D. Lessons to be learned: the molecular basis of kinase-targeted therapies and drug resistance in non-small cell lung cancer. *Angew Chem Int Ed Engl* 2018;**57**:2307–13.
9. Guan X. Cancer metastases: challenges and opportunities. *Acta Pharm Sin B* 2015;**5**:402–18.
10. Jiang H, Deng R, Yang X, Shang J, Lu S, Zhao Y, et al. Peptidomimetic inhibitors of APC-Asef interaction block colorectal cancer migration. *Nat Chem Biol* 2017;**13**:994–1001.
11. Babina IS, Turner NC. Advances and challenges in targeting FGFR signalling in cancer. *Nat Rev Cancer* 2017;**17**:318–32.
12. Touat M, Ileana E, Postel-Vinay S, André F, Soria JC. Targeting FGFR signaling in cancer. *Clin Cancer Res* 2015;**21**:2684–94.
13. Hallinan N, Finn S, Cuffe S, Rafee S, O'Byrne K, Gately K. Targeting the fibroblast growth factor receptor family in cancer. *Cancer Treat Rev* 2016;**46**:51–62.
14. Katoh M. Therapeutics targeting FGF signaling network in human diseases. *Trends Pharmacol Sci* 2016;**37**:1081–96.
15. Helsten T, Elkin S, Arthur E, Tomson BN, Carter J, Kurzrock R. The FGFR landscape in cancer: analysis of 4,853 tumors by next-generation sequencing. *Clin Cancer Res* 2016;**22**:259–67.
16. Parish A, Schwaederle M, Daniels G, Piccioni D, Fanta P, Schwab R, et al. Fibroblast growth factor family aberrations in cancers: clinical and molecular characteristics. *Cell Cycle* 2015;**14**:2121–8.
17. Dienstmann R, Rodon J, Prat A, Perez-Garcia J, Adamo B, Felip E, et al. Genomic aberrations in the FGFR pathway: opportunities for targeted therapies in solid tumors. *Ann Oncol* 2014;**25**:552–63.
18. Hierro C, Rodon J, Tabernero J. Fibroblast growth factor (FGF) receptor/FGF inhibitors: novel targets and strategies for optimization of response of solid tumors. *Semin Oncol* 2015;**42**:801–19.
19. Gozgit JM, Wong MJ, Moran L, Wardwell S, Mohemmad QK, Narasimhan NI, et al. Ponatinib (AP24534), a multitargeted pan-FGFR inhibitor with activity in multiple FGFR-amplified or mutated cancer models. *Mol Cancer Ther* 2012;**11**:690–9.
20. Cheng W, Wang M, Tian X, Zhang X. An overview of the binding models of FGFR tyrosine kinases in complex with small molecule inhibitors. *Eur J Med Chem* 2017;**126**:476–90.
21. Gavine PR, Mooney L, Kilgour E, Thomas AP, Al-Kadhimi K, Beck S, et al. AZD4547: an orally bioavailable, potent, and selective inhibitor of the fibroblast growth factor receptor tyrosine kinase family. *Cancer Res* 2012;**72**:2045–56.
22. Papadopoulos KP, El-Rayes BF, Tolcher AW, Patnaik A, Rasco DW, Harvey RD, et al. A Phase 1 study of ARQ 087, an oral pan-FGFR inhibitor in patients with advanced solid tumours. *Br J Cancer* 2017;**117**:1592–9.
23. Jiang A, Liu Q, Wang R, Wei P, Dai Y, Wang X, et al. Structure-based discovery of a series of 5*H*-pyrrolo[2,3-*b*]pyrazine FGFR kinase inhibitors. *Molecules* 2018;**23**:698.
24. Tucker JA, Klein T, Breed J, Breeze AL, Overman R, Phillips C, et al. Structural insights into FGFR kinase isoform selectivity: diverse binding modes of AZD4547 and ponatinib in complex with FGFR1 and FGFR4. *Structure* 2014;**22**:1764–74.
25. Minor W, Cymborowski M, Otwinowski Z, Chruszcz M. HKL-3000: the integration of data reduction and structure solution-from diffraction images to an initial model in minutes. *Acta Crystallogr D Biol Crystallogr* 2006;**D62**:859–66.
26. Adams PD, Afonine PV, Bunkóczi G, Chen VB, Echols N, Headd JJ, et al. The Phenix software for automated determination of macromolecular structures. *Methods* 2011;**55**:94–106.
27. Murshudov GN, Skubák P, Lebedev AA, Pannu NS, Steiner RA, Nicholls RA, et al. *REFMAC5* for the refinement of macromolecular crystal structures. *Acta Crystallogr D Biol Crystallogr* 2011;**D67**:355–67.
28. Emsley P, Cowtan K. Coot: model-building tools for molecular graphics. *Acta Crystallogr D Biol Crystallogr* 2004;**D60**:2126–32.